Determination of icewine lipids by Ultra High Performance Liquid Tandem Chromatography Quadrupole Time-of-Flight Mass Spectrometry

Jing YANG[1], Kuaile JIANG[1], Peng QU[1], Sibo WAN[2], Qixiu HU[3], Ruzhi MAO[4]*

Abstract

Icewine is a unique food in the world. Lipids in icewine are nutritious and healthy for humans. However, limited studies are available on the qualitative and quantitative analysis of icewine. UPLC-QTOF-MS approach to study lipids in icewine. Bioinformatics strategies will expand the applications of lipidomics in food science,OPLS-DA) was performed to visualise group separation and recognized significantly transform metabolites. In the present study, lipid molecules belonging to 5 classes were qualitatively and quantitatively analysed. The lipids studied were as track: 102 triacylglycerols (TAG), 18 free fatty acids (FFA), 5 diacylglycerols (DAG), 6 ceramides and sphingosine-1-phosphate (Cer), and 1 N-palmitoyl-D-erythro-sphingosylphosphorylc holine (SM). The Shangri-La icewine has higher TAG and FFA content than the Canadian icewine. However, in Canadian icewine samples, the DAG (16:0/16:1) content (398.26 μg/mL) was higher than that of Shangri-La icewine specimens (522.43 μg/mL). The SM (14:0) content in Canadian icewine was higher than that of Shangri-La icewine. UPLC-QTOF-MS is an effective method for detecting lipids in icewine samples. The primary fundamental lipids in icewine samples were TAG, FFA, DAG, Cer, and SM. Therefore, Shangri-La icewine is more nutritious for human health than Canadian icewine.

Keywords: UPLC-QTOF-MS; icewine; lipids; qualitative and quantitative; nutrients and health.

Practical Application: Many thanks to all viticulturists and farmers located in Shangri-La and Pabala Chateau, Heili Chateau, Hada Chateau, Gegu Chateau, Yundin Chateau, Xinwei Chateau for providing the wine samples for the analyses. This study supported by A2032002451 and KX142021090 of Yunnan Agricuture University.

1 Introduction

Lipids are globally accessible with a strong effect and honour in food science. Recently, mass spectrometry (MS) was used to study of food lipids and research on dietary lipid nutrition within foodomics, which brings several strategies to provide novel insights into lipid nutrition and human health. MS-based platforms, and chemometric as effective tools used in lipidomics research, food health benefits food lipids traceability (Wu et al., 2021). Lipids composition and components easily determination by MS-based analysis. When combined with chemometric equipment, MS-based lipidomics analysis enables the sensitive of concerning lipid molecules, investigation the functional roles of wine lipids. MS-based lipidomics in foodomics research provided more knowledge on food lipids (Li et al., 2021; Siriwardane et al., 2020) .Lipidomics is a mighty approach that can provide a quantitative characterisation of manyquiet few lipids from biological samples. Lipidomics studies focus on mysterious biology (Macrae et al., 2013). Lately, MS-based 'shotgun lipidomics' has been a powerful tool for quantitative and qualitative analysis of complicated lipids food matrics.

Wine is frequent consumed as food. It affords energy for crucial fatty acids for the body. Icewine, a unique natural and favourite wine, can be produced in cold and harsh Germany, Canada, and China.Lipids in icewine are aromatic in nature. Moreover, energy storage and energy supply are the most urgent physiological functions of lipids (Fragopoulou et al., 2000). Lipid is one of the essential nutrients necessary to the human body (Nagayama & Katsuta, 2014). Cholesterol ester, which reduces cholesterol and triglycerides in the blood (Wu et al., 2021).

Lipids are an essential nutrient and flavour substance in icewine, which originate from wine fermentation and vintage process. An untargeted lipidomics profiling approach based on ultraperformance liquid chromatography–time-of-flight tandem MS was successfully used to study the origin of commercial Pinot noir wines (Phan & Tomasino, 2021).Such as, linolenic acid in grape juice significantly affected the formation of volatile thiols, thus giving a tropical fruit flavour to the wine (Srisamatthakarn, 2011). Therefore, grape lipids are essential for *Saccharomyces cerevisiae* during ethanol fermentation, and free fatty acids (FFA) in grape mash also affect the formation of volatile substances (Li et al., 2022). The tolerance of yeast to ethanol, acetic acid, and acetaldehyde is closely related to the lipid composition of the cell membrane (Ghareib et al., 1988).

No qualitative and quantitative studies on lipids in icewine are available. Therefore, the current study aimed to comprehensively detecting the lipids in icewine from different regions using lipidomics technology to understand differences between the lipid composition of icewine from the different areas and deepen the existing understanding of lipid in icewine.

In the present study, the identification, quantitative analysis, and comparison of lipids in icewine from different regions, such as Canada and Shangri-La, was performed. Lipids in the icewine indicates food nutrients are beneficial to human health.

2 Materials and methods

2.1 Sample collection

C-2016 (N = 6) was purchased from 6 Canadian icewine chateaux, and Y-2016 (N = 6) was collected from 6 icewine enterprises chateaux from Shangri-La of Yunnan, China. The wine bottles were immediately stored at −80 °C until further use (Supplementary Material).

2.2 Metabolite extraction

500 μL of each icewine sample from 6 Canadian icewine chateau and 6 Icewine Enterprises chateaux were transferred to an Eppendorf tube, and subsequently a 1200-μL extract solution (methyl tertiary butyl ether (MTBE): MeOH = 5:1) containing an internal standard was added. After vortexing for 60 s, the samples were sonicated for 10 min in an ice-water bath. Then the samples were centrifuged at 3000 rpm for 15 min at 4 °C. The supernatant of 900 μL was removed to a fresh tube. The rest of the sample was combined with 900 μL of MTBE, followed by vortexing, sonication, and centrifugation. Again, 900 μL of the supernatant was removed. The step was repeated twice. All supernatants were mixed and dried in a vacuum concentrator at 37 °C. Then, the dried samples were transferred in a 200-μL resuspension buffer (dichloromethane:MeOH: H_2O = 60:30:4.5) by sonication in ice for 10 min. The mixture was then centrifuged at 12000 rpm for 15 min at 4 °C, and 30 μL of the supernatant was transferred to a fresh cup vial for liquid chromatography (LC)/MS analysis. Quality control samples were prepared by mixing an equal aliquot of the supernatants from all samples.

2.3 LC-MS/MS analysis

The ultra-high performance liquid chromatography (UHPLC) separation was performed using the SCIEX ExionLC series UHPLC System. The AB SCIEX QTrap 6500+ mass spectrometer was used for assay development. The mobile phase A constitutes of 60% acetonitrile, 10 mmol/L ammonium formate, and 40% water; the mobile phase B consisted of 90% isopropanol, 10% acetonitrile, and 10 mmol/L ammonium formate. The column temperature was 40 °C; the injection volume was 2 μL, and the auto-sampler temperature was 6 °C. Typical ion source parameters were as follows: IonSpray voltage: +5500/-4500 V, curtain gas: 40 psi, temperature: 350 °C, ion source gas 1:50 psi, ion source gas 2: 50 psi, DP: ± 80 V.

2.4 Data pre-processing and annotation

Peak area of QC samples and The TIC retention time overlap well, indicating that LC-MS/MS system has good stability (Figure 1). TIC diagram of positive and negative ion modes of QC and blank samples. Through the detection of blank samples, the material residue in the detection process can be investigated. There is no manifest interference peak detected in blank samples relative to QC samples, indicating that the material residue is effectively

controlled and there is no obvious cross-contamination between samples (Figure 2). Lipids compounds were quantification by Skyline 20.1 Software.The internal standard (IS) was using the absolute content of individual lipids was calculated, which based on peak area and the actual concentration of the identical lipid class IS, and then the absolute content was obtained from the diverse IS averaged of the identical lipid class (Dunn et al., 2011; Tu et al., 2017; Want et al., 2010). 154 peaks were detected in the current study, and 142 metabolites remained after relative standard deviation de-noising. The missing values were then filled up by half of the minimum value. Additionally, the normalisation method was used to analyse data. The final data including the peak number, sample name, and normalised peak area was inputted to the SIMCA16.0.2 software package (Sarus Stedimtoritics Data AB, Umea, Sweden) for multivariate analysis. Data were scaled and logically transformed to minimise the effect of noise and high variance of the variables. After these transformations, principal component analysis (PCA), an unsupervised analysis that reduces the dimension of the data, was performed to visualise the distribution and grouping of the samples. Supervised orthogonal projections to latent structuralism-discriminated analysis (OPLS-DA) were performed to visualise group separation and identify significantly changed metabolites. R2 and Q2 values to assess robustness of the model, the risk of overfitting, and the reliability of the model (Boccard & Rutledge, 2013).The metabolites with the value of variable importance in the projection (VIP) > 1 and p < 0.05 (student t-test) were considered as significantly changed metabolites. In the appendix, commercial databases, including Kyoto Enmyeons paedia of Genes and Genomes (http://www.genome.jp/kegg/) and Metaboanalyst (https://www.metaboanalyst.ca/) were used for pathway enrichment analysis (Chong et al., 2018).
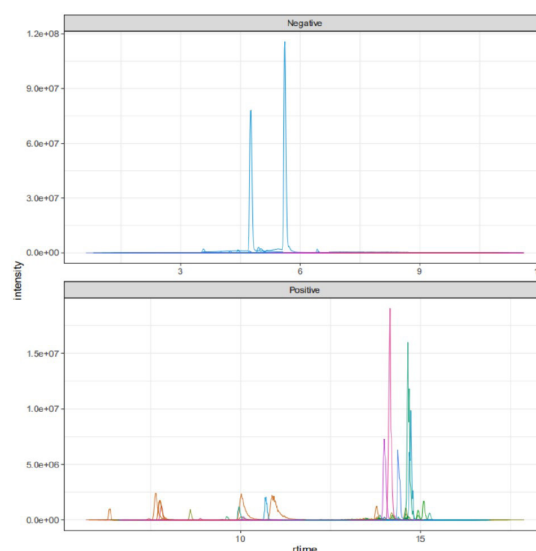
Figure 1. UHPLC-QTOF-MS detection of QC samples Total extraction ion flow diagram of positive and negative ion modes, The UHPLC separation was carried out using a SCIEX ExionLC series UHPLC System. AB Sciex QTrap 6500+ mass spectrometer was applied for assay development. Typical ion source parameters were: IonSpray Voltage: +5500/-4500 V, Curtain Gas: 40 psi, Temperature: 350ºC, Ion Source Gas 1:50 psi, Ion Source Gas 2: 50 psi, DP: ±80V.

3 Result

3.1 Multivariate analysis

In this study, PCA was used modeling all samples. Figure 3a, 3b show C2016, Y-2016 and QC samples, PC1 (37.2%) and PC2 (16.8%), the samples were all within the 95% confidence interval,

the results are reliable. The ordinate t[1]P in the score scatter plot of OPLS-DA model for group C-2016 vs. Y-2016 indicates the predicted principal component score of the first principal component, showing the difference between groups of samples. The ordinate t[1]O indicates the score of the orthogonal principal component 2, showing the difference within the sample group.
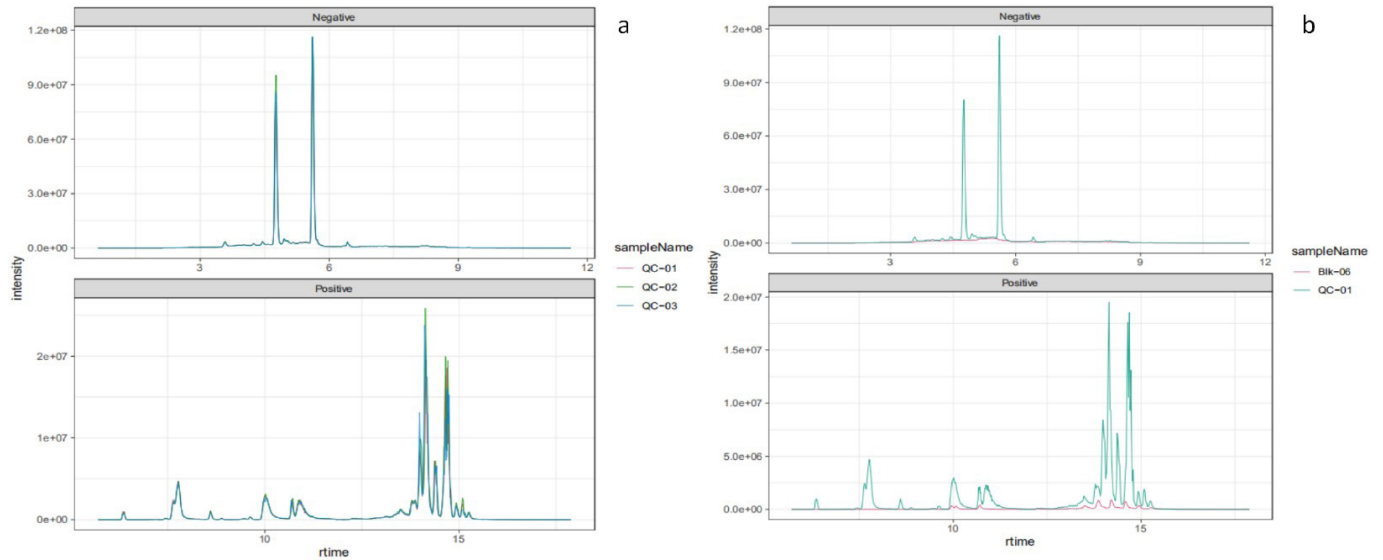
Figure 2. 2a: TIC diagrams of positive and negative ions of all QC samples. The detection of the sample lasted for a long time, especially the real time monitoring of the stability of the instrument and the normal signal during the detection process. Discover anomalies in time and eliminate problems as soon as possible to ensure the quality of final data collection. The TIC retention time and peak area of QC samples overlap well, indicating that the instrument has good stability. 2b: TIC diagram of positive and negative ion modes of QC and blank samples. Through the detection of blank samples, the material residue in the detection process can be investigated. There is no obvious interference peak detected in blank samples relative to QC samples, indicating that the material residue is effectively controlled and there is no obvious cross-contamination between samples.
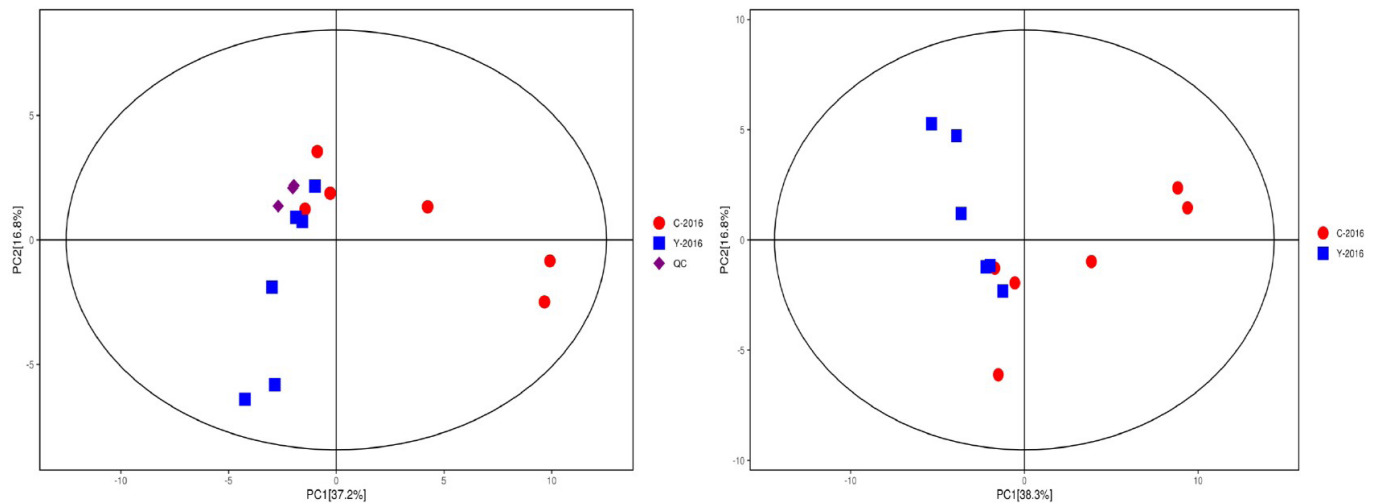
Figure 3. 3a: Score scatter plot for PCA model TOTAL with QC for all samples. The abscissa PC and the ordinate PC represent the scores of the first and second principal components, respectively. Each scatter represents a sample and the color and shape of the scatter represent different groupings. The samples are all within the 95% confidence interval (Hotelling's T-squared ellipse). 3b: Score scatter plot of PCA model for group C2016 vs. Y-2016 in group C-2016 The results of PCA score plot show that all samples are within the 95% confidence interval (Hotelling's T-squared ellipse).
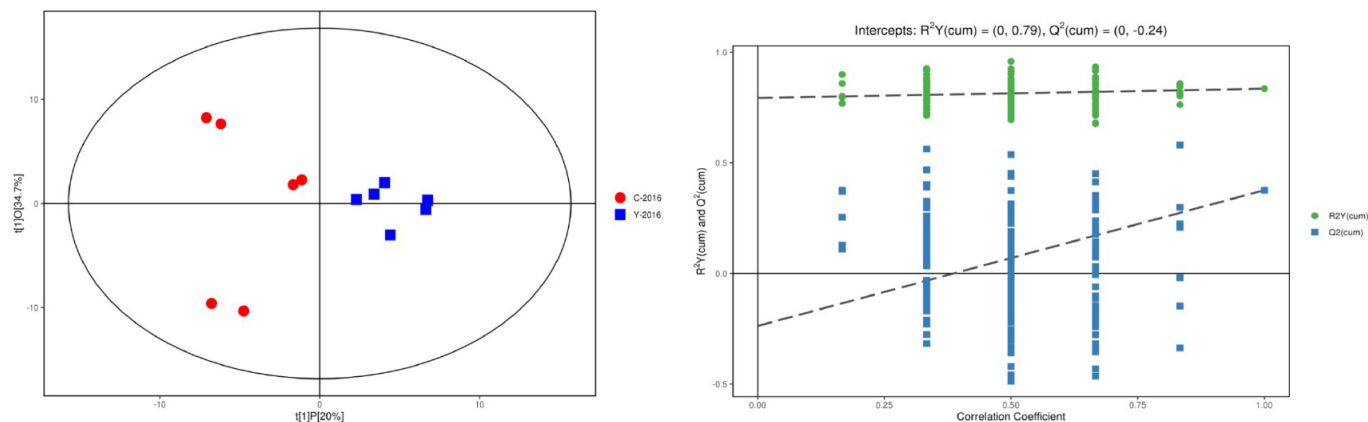
Figure 4. 4a: ln the score scatter plot of OPLS-DA model for group C-2016 vs Y-2016 of the Y-2016 group, the abscissa t P in the score scatter plot of OPLS-DA model for group C-2016 vs Y-2016 indicates the predicted principal component score of the first principal component, showing the difference between groups of samples. The ordinate t O indicates the score of the orthogonal principal component 222222, showing the difference within the sample group. Each scatter represents a sample, and the shape and color of the scatter indicate different experimental groups. From the results of OPLS-DA score chart, it can be seen that the two groups of samples are very distinct, and all samples are in the 95% confidence interval (Hotelling's T-squared ellipse). 4b: The permutation test results of the OPLS-DA model of the Y-2016 group in the C-2016 group (Permutation test of OPLS-DA model for group C-2016 vs Y-2016) show that the abscissa represents the permutation retention of the permutation test (the proportion consistent with the original model Y variable sequence, and the point where the permutation retention is equal to 1 is the RY and Q values of the original model), the ordinate represents the value of RY or Q, the green dot represents the RY value obtained by the permutation test, and the blue square point represents the Q value obtained by the permutation test. The two dashed lines represent the regression lines of RY and Q, respectively. Toe original model RY is very close to 1, indicating that the established model conforms to the real situation of the sample data; the intercept between the regression line of Q and the longitudinal axis is less than zero; at the same time, as the replacement retention decreases gradually, the proportion of Y variable increases, and the Q of the random model decreases gradually. It shows that the original model has good robustness and there is no overfitting phenomenon.

From the results of OPLS-DA score chart, it can be seen that the two groups of samples were extremely distinct, and all samples are in the 95% confidence interval (Hotelling's T-squaredcurve se). The permutation test results of the OPLS-DA model of the Y-2016 group in the C-2016 group show that the abscissa represents the permutation retention of the permutation test, the original model RY is very close to 1, indicating that the established model conforms to the real situation of the sample data ; the intercept between the regression line of Q and the amount of time, longitudinal axis is less than zero ; at the equal time, as the replacement retention decreases gradually, the proportion of Y variable increases, and the Q of the random model decreases gradually. It shows that the original model has good robustness and there is no overfitting phenomenon (Figure 4a, 4b). In the heatmap of hierarchical clustering analysis for group C-2016 vs Y-2016, the ordinate represents the differential metabolites compared to the group, the color blocks at different positions represent the relative expression of metabolites at corresponding positions, the red represents the high expression of the substance content, and the blue represents the low expression of the substance content (Figure 5). The horizontal and vertical coordinates in the Heatmap of correlation analysis for group C-2016vs Y-2016 diagram of the C-2016 group for Y-2016 group standy for differential metabolites in this group. The color blocks at different positions represent the correlation coefficient among the metabolites at the corresponding positions. Red represents a positive correlation, and blue represents a negative correlation (Figure 6).
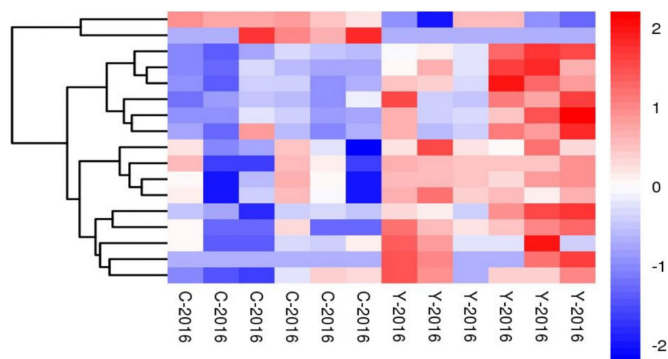
Figure 5. ln the Heatmap of hierarchical clustering analysis for group C-2016 vs Y-2016, the abscissa represents different experimental groups, the ordinate represents the differential metabolites compared with the group, the color blocks at different positions represent the relative expression of metabolites at corresponding positions, the red represents the high expression of the substance content, and the blue represents the low expression of the substance content.

3.2 Univariate analysis

Screening of differential metabolites in group Y-2016 Volcano plot for group C-2016 (Volcano plot for group C-2016 vs Y-2016) Volcano plot showed that each point represented a metabolite, the abscissa represented the multiple changes of each substance in the group (taking the logarithm of the bottom 2), ordinate represented the P-value of the student

Figure 6. The horizontal and vertical coordinates in the Heatmap of correlation analysis for group C-2016 vs Y-2016 diagram of the C-2016 group for Y-2016 group represent the differential metabolites in this group. The color blocks at different positions represent the correlation coefficient between the metabolites at corresponding positions. The red represents a positive c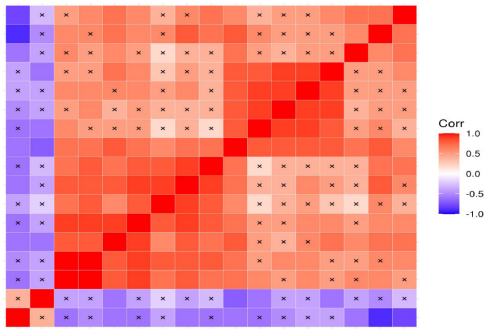orrelation, and the blue represents a negative correlation. The deeper the color is, the stronger the correlation is. At the same time, the non-obviousness correlation is marked with a fork.
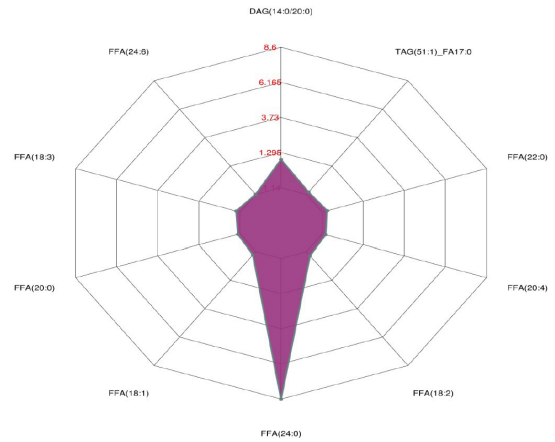

Figure 7. Screening of differential metabolites in group Y-2016 Volcano plot for group C-2016 (Volcano plot for group C-2016 vs Y-2016) Volcano plot showed that each point represented a metabolite, the abscissa represented the multiple changes of each substance in the group (taking the logarithm of the bottom 2), the ordinate represented the P-value of the student t test (taking the negative number of the bottom 10), and the scatter size represented the VIP value of the OPLS-DA model. The larger the scatter, the greater the VIP value. The scatter color represents the final screening results. The up-regulated metabolites are red, the down-regulated metabolites are blue, and the nonsignificant metabolites are gray.

Figure 8. Radar chart analysis for group C-2016 vs Y-2016 in group C-2016 (C-2016 vs Y-2016). We calculated the corresponding ratio of the quantitative value of differential metabolites, and took the logarithmic transformation with 2 as the bottom. The figure was represented by red font, and each grid line represented a difference multiple. The purple shadow was composed of the difference multiple connections of each substance, and the corresponding content trend changes were shown in the radar chart.
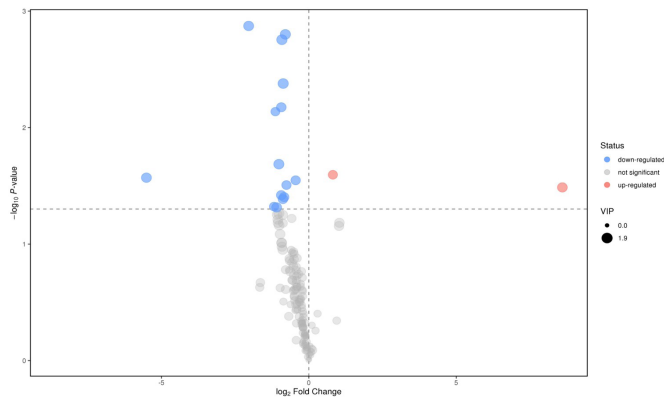

Figure 9. Each column in the Bar plot for group C-2016 vs Y-2016 lipid profile represents a class of metabolites. The ordinate of the figure represents the relative change percentage of each substance content in this group. If the relative change percentage of the content is zero, it means that the content of the substance in the two groups is the same; the percentage of relative content change was positive, indicating that the content of the substance was higher in the C-2016 group; the relative percentage change of content was negative, indicating that the substance was higher in the Y-2016 group. The transverse coordinates of the lipid group histogram represent the classification information of lipids.

t test (taking the negative number of the bottom 10), and the scatter size represented the VIP value of the OPLS-DA model. The larger the scatter, the greater the VIP value. The scatter color represents the screening results. The upregulated metabolites are red, the downregulated metabolites are blue, and the nonsignificant metabolites are gray (Figure 7).

Radar map analysis for C-2016 vs Y-2016. We calculated the corresponding ratio of the quantitative value of differential metabolites, the figure was represented by red font, and each grid line represented the difference multiple. The purple shadow was composed of the difference between the difference between multiple connections of each substance, and the corresponding content trends were shown in the radar chart (Figure 8).

Each column in the bar plot for group C-2016 vs Y-2016 lipid profile represents a class of metabolites. The ordinate of the figure represents the relative change percentage of each substance content in this group. If the relative change percentage of the content is zero, it means that the content of the substance in the two groups is the same; the percentage of relative content change was positive, indicating that the content of the substance was higher in the C-2016 group; the relative percentage change of content was negative, indicating that the substance was higher in the Y-2016 group. The transverse coordinates of the lipid group histogram represent the class information of lipids (Figure 9).

Bubble plot for group C-2016 vs Y-2016. Each point in the bubble plot represents a metabolite. The size of the point represents the P-value of the Student t-test (negative number of arithmetic ms based on 10), and the larger point represents, the minor the P-value. Gray points represent nonindigenous differences with P-value not less than 0.05, and color points represent indigenous differences with P-value less than 0.05 (marked by different colors according to lipid classification).

The transverse coordinates of the bubble diagram of the lipid group represent the relative percentage of the content of each substance in the group (for the substance with a great change in in content, the relative change percentage of its content is directly marked on its point, and the relative change percentage of its content is the corresponding abscis scale). The relative change percentage of the content is zero, indicating that the content of the substance in the two groups is the same ; the percentage of relative content was positive, indicating that the content of the substance was higher in the C-2016 group ; the relative percentage change of content was negative, indicating that the substance was higher in the Y-2016 group. The ordinate of the bubble diagram of lipid group represents the class information of lipid. The black line at the bottom shows the distribution density of metabolites (one line represents a metabolite) (Figure 10).

3.3 Lipids composition in Icewine

In the present study, LC-QTOF-MS detected 154 lipids belonging to 5 classes, found 142 effective lipids,namely, 112 TAGs, 18 FFAs, 5 DAGs, 6Cers, and 1 SM in icewine samples(Table 1). Just 17 lipids, namely 1 DAG, 8 FFA, and 8 TAG, were differentially expressed metabolites between Shangri-La and Canadian icewine samples;Total Canadian (5105.59 µg/mL) icewine samples' TAG content was higher than Shangri-La's (6291.11 µg/mL); FFA (14:0), FFA (20:0), FFA(18:2), FFA (22:1), DAG (16:0/18:0), TAG (48:0)_FA16:0, TAG (50:0)_FA16:0, TAG (52:0)_FA18:0, FFA (16:1), DAG (16:0/16:0), TAG (54:0)_FA18:0, TAG (50:0)_FA18:0, FFA (22:0), TAG (52:0)_FA16:0, TAG (46:0)_FA16:0, and TAG (47:0)_FA16:0 content of more than 10 µg/mL and FFA (18:0), FFA (16:0), and FFA (18:1) of more than 100 µg/mL were the main lipids both in Shangri-La and Canadian icewine samples; Varities lipids and could be predicting wine origin (Phan & Tomasino, 2021), in this study, only 17 lipids as markers of Shangri-La's icewine, such as TAG content was higher than Shangri-La's (6291.11 µg/mL). FFA (14:0), FFA (20:0), FFA(18:2), FFA (22:1), DAG (16:0/18:0), TAG (48:0)_FA16:0, TAG (50:0)_FA16:0, TAG (52:0)_FA18:0, FFA (16:1), DAG (16:0/16:0), TAG (54:0)_FA18:0, TAG (50:0)_FA18:0, FFA (22:0), TAG (52:0)_FA16:0, TAG (46:0)_FA16:0, and TAG (47:0)_FA16:0 content of more than 10 µg/mL and FFA (18:0), FFA (16:0), and FFA (18:1) (Table 2). Among 112 TAG molecular species, merely TAG (48:1) (7.14 µg/mL vs 10.59 µg/mL), TAG (52:2)_FA16:1 (1.07 µg/mL vs 2.43 µg/mL), TAG (51:3), FA18:2 (0.46 µg/mL vs 0.85 µg/mL), TAG (54:2)_FA18:2 (0.46 µg/mL vs 0.63 µg/mL), TAG (46:1)_FA16:0 (4.21 µg/mL vs 5.70 µg/mL), TAG (50:2)_FA14:0 (0.23µg/mL vs 0.73µg/mL), TAG (44:1)_FA14:0 (2.18µg/mL vs 2.88µg/mL), TAG (44:0)_FA18:0 (0.33 µg/mL vs 0.58 µg/mL), and TAG (48:1)_FA16:1 (7.14 µg/mL vs 10.59 µg/mL) in Canadian icewine were significantly higher than in Shangri-La icewine; Most of the TAG molecular species content was not significantly different between the 2 samples, accounting for less than 32.27 µg/mL; Total Canadian (398.26 µg/mL) icewine samples' TAG content was higher than Shangri-La icewine samples (522.43 µg/mL) (Table 3). TAG (52:2)_FA16:1, TAG (48:1), FA16:1, TAG

Figure 10. Bubble plot for group C-2016 vs Y-2016. Each point in the Bubble plot represents a metabolite. The size of the point represents the P value of the student t test (negative number of logarithms based on 10), and the larger the point represents the smaller the P-value. Gray points represent non-indigenous differences with P-value not less than 0.05, and color points represent indigenous differences with P-value less than 0.05 (marked by different colors according to lipid classification).

(46:1)_FA16:0 as an adjuvant can be the main contributor to the toxicity of a mixture of 2 organophosphorus pesticides with relatively low toxicity in fish cells (Olsvik & Søfteland, 2020). TAG54:2FA18:1 in combination with LPE (16:0) and PE (16:0/20:2) can be used to distinguish between healthy people and type-2 diabetics or healthy people and early diabetic nephropathy. TAG (44:0)_FA18:0 were preserved in the absence of free fatty acids, basic respiration rates, and phosphorylating efficiency of mitochondria.

Eighteen FFA molecular species, namely FFA (18:0) (2551.46 µg/mL vs 356.00 µg/mL), FFA (14:0) (61.24 µg/mL vs 15.34 µg/mL), FFA (22:1) (31.37 µg/mL vs 10.01 µg/mL), FFA (16:1) (61.24 µg/mL vs 8.12 µg/mL), FFA (20:1) (7.43 µg/mL vs 3.27 µg/mL), FFA (20:2) (0.29 µg/mLvs 0.12 µg/mL), and FFA (26:0) (4.19 µg/mL vs 3.52 µg/mL), was not significantly different between Canadian and Shangri-La icewine. Eight FFA molecular species, namely, FFA (24:6) (1.21 µg/mL vs 0.60 µg/mL), FFA (18:3) (3.05 µg/mL vs 0.59 µg/mL), FFA (20:0) (31.37 µg/mL vs 10.01 µg/mL), FFA (18:1) (111.26 µg/mL vs 25.78 µg/mL), FFA (24:0) (11.90 µg/mL vs 9.92 µg/mL), FFA (20:4) (0.65 µg/mL vs 0.17 µg/mL), FFA (22:0) (10.06 µg/mL vs 5.10 µg/mL), and FFA (18:2) (10.06 µg/mL vs 5.10 µg/mL) were significantly higher in Canadian icewine than in Shangri-La icewine. Total Canadian (4566.15 µg/mL) icewine samples' FFA content was higher than that of Shangri-La icewine (706.37 µg/mL) (Table 4). FFA (18:1), FFA (16:0) were the main lipid in both classes of wines. Sodium (Na) infusion in rats produces FFA rebound and insulin resistance. A case of electrolyte disturbance and seizure secondary to the rectal administration of 2 fleet paediatric enemas and smaller increase in plasma FFA level, infused for 2 h (0.1 γ/kg/min) induced a much more significant rise in plasma FFA and blood glucose levels in obese mice than in healthy subjects (Youngtaek et al., 1986). FFA (18:3): Machado-Joseph disease (SCA3/MJD) is a rare autosomal dominant neurodegenerative disease resulted in by an abnormal expansion of CAG repeats in the ATXN3 gene. A series of essays on human vascular endothelial cells exposed to

Table 1. Lipids molecular species in icewine samples.

Class	CompoundName	RT	Q1	Q3	C-2016-1-1	C-2016-2-1	C-2016-3-1	C-2016-4-1	C-2016-5-1	C-2016-6-1	QC-01	QC-02	QC-03	Y-2016-1-1	Y-2016-2-1	Y-2016-3-1	Y-2016-4-1	Y-2016-5-1	Y-2016-6-1
CER	Cer(18:1/16:0)-IS	8.60	547.58	264.40	1000	1000	1000	1000	1000	1000	1000	1000	1000	1000	1000	1000	1000	1000	1000
CER	Cer(18:1/26:1)	11.92	676.60	264.26	25.89	19.58	22.46	15.20	10.04	10.68	23.93	24.09	23.76	25.48	17.63	18.46	27.04	10.18	19.59
CER	Cer(18:1/26:0)	12.29	678.60	264.26	19.90	23.79	24.43	12.72	9.12	12.16	22.20	22.26	22.58	25.01	17.12	11.17	29.92	13.18	21.82
CER	Cer(18:1/22:0)	10.94	622.60	264.26	10.67	7.65	6.58	7.42	4.54	3.07	10.02	9.34	8.49	8.68	10.08	7.19	13.65	7.04	6.50
CER	Cer(18:1/24:0)	11.65	650.60	264.26	35.01	24.25	25.45	23.39	16.52	13.13	33.42	32.11	37.86	34.57	27.62	21.37	41.09	22.08	26.07
CER	Cer(18:1/16:1)	8.25	536.50	264.26	11.68	6.20	9.82	16.62	4.78	5.48	17.20	15.53	13.36	18.00	12.58	6.60	23.09	5.59	10.35
CER	Cer(18:1/24:1)	11.25	648.60	264.26	21.42	18.07	20.37	16.93	11.25	10.00	25.19	22.03	30.30	23.71	14.91	19.07	32.20	13.45	19.25
DAG	DAG(15:0/18:1)-IS	9.62	605.51	299.20	500	500	500	500	500	500	500	500	500	500	500	500	500	500	500
DAG	DAG(16:0/16:1)	9.38	584.40	313.20	24.90	26.35	20.34	14.05	8.98	NA	24.68	24.41	24.34	23.24	39.32	14.21	21.59	15.09	21.06
DAG	DAG(16:0/16:0)	9.96	586.50	313.30	2606.74	2407.49	2476.78	2382.82	2452.21	2399.33	2084.59	2037.12	2066.14	NA	NA	2369.38	NA	2295.96	2510.83
DAG	DAG(14:0/20:0)	10.70	614.60	285.20	13.33	11.56	10.52	12.82	12.61	12.41	10.18	9.79	9.53	5.88	5.93	17.86	4.55	12.01	11.75
DAG	DAG(16:0/18:0)	10.70	614.40	313.20	4870.18	3750.83	3481.88	4485.32	4220.42	3590.92	3738.00	3936.00	3522.89	NA	NA	4155.04	NA	3712.08	4138.30
DAG	DAG(16:1/16:1)	8.79	582.40	311.20	17.28	20.06	18.17	9.46	6.37	5.16	15.39	24.82	16.41	14.46	17.11	10.15	15.13	9.10	6.77
FFA	FFA(16:0)-IS	4.72	264.29	264.29	2181.13	2055.88	1972.84	1912.06	2139.34	1937.43	2042.91	2018.48	2036.21	2129.82	2207.68	2033.36	2306.12	1862.48	1891.73
FFA	FFA(17:1)-IS	4.44	267.23	267.23	2928.07	3188.88	3411.62	3610.06	3006.92	3522.96	3220.59	3283.24	3237.37	3025.94	2881.55	3244.62	2729.47	3801.10	3684.82
FFA	FFA(24:6)	4.73	355.30	355.30	72.01	82.84	73.68	74.33	744.89	59.07	164.50	167.97	165.71	110.64	178.00	103.30	185.60	144.45	76.33
FFA	FFA(18:0)	5.58	283.20	283.20	115428.83	129530.06	117088.10	148063.91	148913.14	106414.40	222615.98	219236.85	228028.09	200962.05	326147.59	159231.04	338238.32	229285.36	167439.23
FFA	FFA(18:3)	3.54	277.20	277.20	134.04	154.42	150.63	170.19	196.45	110.46	248.72	253.41	260.30	227.25	380.86	276.47	279.90	363.54	198.19
FFA	FFA(20:0)	6.41	311.20	311.20	1608.42	1694.27	1845.80	2387.90	2660.11	1542.61	3434.26	3416.45	3267.44	3938.83	5171.83	2332.48	6152.38	3701.90	2464.28
FFA	FFA(14:0)	3.57	227.10	227.10	2661.33	2680.41	3853.78	3941.61	3265.04	1970.33	4431.50	4645.91	4406.16	3906.19	4888.94	4645.74	7891.82	6316.92	4536.30
FFA	FFA(18:1)	4.95	281.20	281.20	4666.71	6451.79	6139.31	7023.14	5596.18	3501.35	9538.79	9440.11	10039.91	7600.04	13272.00	8333.50	12695.86	11996.66	7135.12
FFA	FFA(16:0)	4.76	255.10	255.10	74794.12	96393.37	84541.28	97338.64	82923.93	64626.09	156589.42	167399.99	165148.93	113437.58	187119.81	116873.28	227652.11	128405.26	104455.78
FFA	FFA(22:1)	6.45	337.30	337.30	1494.05	2017.96	1126.11	1822.63	2093.75	855.86	1570.06	1548.92	1462.11	2450.69	5196.11	2774.47	3485.03	3989.37	2340.47
FFA	FFA(16:1)	4.01	253.10	253.10	1216.41	965.44	1429.66	2073.83	1546.92	1043.79	1503.06	1414.53	1526.79	1327.53	1691.26	1672.59	2172.11	2766.70	1605.68
FFA	FFA(24:6)	8.28	367.30	367.30	NA	604.91	1107.68	781.83	1072.48	NA	1137.68	1073.64	NA	NA	NA	NA	NA	NA	NA
FFA	FFA(20:5)	3.84	301.20	301.20	190.80	178.49	229.65	201.68	191.03	208.16	204.00	199.46	185.59	159.49	246.70	136.22	275.54	374.06	158.47
FFA	FFA(28:0)	10.16	423.30	423.30	58.55	47.20	130.78	56.95	67.32	NA	87.88	79.45	82.75	156.01	123.95	65.02	164.25	93.18	65.02
FFA	FFA(18:2)	4.25	279.20	279.20	1450.25	1421.44	1679.28	1868.86	1875.94	1120.37	1987.49	1775.07	1983.81	2510.31	3115.75	2468.39	2765.03	3610.00	1889.32
FFA	FFA(20:4)	4.06	303.20	303.20	21.92	27.26	44.95	35.99	36.98	28.78	40.97	44.15	37.32	80.42	62.57	39.68	83.08	71.04	37.75
FFA	FFA(20:1)	5.69	309.20	309.20	375.18	544.68	272.55	341.69	561.63	132.78	296.50	240.56	269.21	246.27	1281.65	606.76	335.24	751.94	466.01
FFA	FFA(22:0)	7.32	339.30	339.30	435.04	358.26	477.87	493.42	992.40	259.55	589.19	690.79	727.34	923.01	990.66	500.92	1338.19	1093.14	551.77
FFA	FFA(20:2)	5.23	307.20	307.20	14.53	19.00	23.04	15.57	9.35	6.77	23.99	23.26	18.14	27.51	48.87	18.57	37.78	24.05	19.55
FFA	FFA(26:0)	9.24	395.30	395.30	242.13	226.91	384.46	NA	399.66	NA	508.39	333.92	342.55	NA	NA	NA	1075.58	645.21	NA
SM	SM(16:0)-IS	7.63	710.62	184.20	1771.30	1683.95	1835.30	1790.64	1784.53	1774.66	1811.09	1801.57	1813.43	1776.18	1743.85	1802.77	1754.40	1778.20	1813.75
SM	SM(18:1)-IS	7.75	738.58	184.07	1300.85	1330.39	1276.02	1319.81	1270.73	1291.78	1287.88	1261.81	1263.78	1315.39	1312.56	1293.05	1316.52	1296.79	1246.04
SM	SM(24:1)-IS	10.03	820.73	184.20	2671.41	2706.65	2630.54	2575.78	2721.39	2657.77	2624.93	2688.11	2684.24	2649.38	2630.76	2553.90	2620.84	2625.77	2767.26
SM	SM(24:0)-IS	10.90	822.74	184.20	3420.17	3508.28	3432.92	3382.69	3506.11	3494.89	3443.34	3566.22	3511.98	3340.97	3514.12	3566.65	3461.75	3500.71	3511.91
SM	SM(14:0)	6.35	675.50	184.10	472.43	329.26	508.30	356.58	424.98	354.48	454.06	391.42	388.76	279.66	335.72	425.39	426.27	445.78	366.24
TAG	TAG(48:1/FA18:1)-IS	13.79	829.72	523.48	2750.00	2750.00	2750.00	2750.00	2750.00	2750.00	2750.00	2750.00	2750.00	2750.00	2750.00	2750.00	2750.00	2750.00	2750.00

Table 1. Continued...

Class	CompoundName	RT	Q1	Q3	C-2016-1-1	C-2016-2-1	C-2016-3-1	C-2016-4-1	C-2016-5-1	C-2016-6-1	QC-01	QC-02	QC-03	Y-2016-1-1	Y-2016-2-1	Y-2016-3-1	Y-2016-4-1	Y-2016-5-1	Y-2016-6-1
TAG	TAG50:0-FA18:0	14.59	852.80	551.50	974.41	820.89	949.97	2285.05	714.88	959.00	1188.14	1214.01	1213.32	930.48	875.95	1148.56	1041.88	823.63	1034.34
TAG	TAG51:0-FA17:0	14.75	866.80	579.50	61.14	70.44	86.55	91.48	27.13	42.04	83.33	85.52	83.77	78.40	74.90	68.34	92.65	56.95	46.30
TAG	TAG47:1-FA17:0	13.55	808.70	521.40	63.06	66.53	85.80	85.64	33.36	32.05	68.79	69.68	67.76	78.70	48.31	59.43	76.17	40.49	46.91
TAG	TAG49:0-FA18:0	14.39	838.80	537.50	116.27	125.93	160.02	147.50	66.97	48.87	138.78	140.37	143.05	143.62	122.71	128.21	118.13	96.10	86.94
TAG	TAG52:0-FA18:0	14.93	880.80	579.50	2032.31	1772.30	2095.48	3428.81	1774.37	2004.36	1949.05	2045.10	2042.08	1531.66	1283.73	2127.91	1507.13	1754.61	1973.45
TAG	TAG48:1-FA16:1	13.85	822.70	551.40	468.05	447.06	675.40	549.52	261.75	238.60	614.03	636.96	603.63	554.39	462.88	527.00	493.70	567.12	570.64
TAG	TAG44:0-FA18:0	13.36	768.71	467.41	27.48	23.53	44.64	NA	NA	NA	NA	33.41	34.94	34.56	50.75	31.25	26.00	NA	29.04
TAG	TAG44:1-FA14:0	12.89	766.69	521.46	127.26	99.34	184.40	122.91	57.37	63.47	162.28	152.34	158.83	135.57	148.52	153.70	149.42	117.50	160.76
TAG	TAG50:1-FA18:1	14.20	850.80	551.50	655.01	NA	838.56	NA	NA	NA	NA	733.07	768.49	NA	NA	NA	NA	NA	NA
TAG	TAG46:0-FA16:0	13.79	796.70	523.47	886.24	663.48	910.99	1160.96	439.14	467.94	872.34	938.25	915.44	799.93	834.29	782.69	793.45	644.65	697.59
TAG	TAG47:1-FA14:0	13.59	808.70	563.50	100.97	85.40	163.59	130.69	70.84	72.91	169.11	168.81	157.83	133.21	123.70	129.71	110.28	104.15	154.04
TAG	TAG45:0-FA16:0	13.56	782.72	509.46	374.55	342.74	476.40	523.58	235.36	227.54	428.32	456.36	425.59	421.85	424.36	449.47	401.23	326.10	445.01
TAG	TAG50:0-FA16:0	14.59	852.80	579.50	1835.83	1514.29	1739.24	5092.01	1309.68	1623.45	2193.16	2157.62	2364.15	1632.70	1694.72	2009.04	2156.55	1371.12	1924.53
TAG	TAG54:0-FA16:0	15.26	908.80	635.50	93.45	89.70	108.60	119.93	59.33	58.25	99.28	106.97	109.32	96.70	77.92	87.51	97.20	72.20	74.74
TAG	TAG52:3-FA16:1	13.84	874.80	603.50	NA	NA	NA	NA	NA	NA	183.91	197.52	NA	231.35	261.23	NA	NA	NA	NA
TAG	TAG48:0-FA16:0	14.20	824.70	551.40	1649.42	1546.00	1977.32	3754.20	1139.15	1312.79	1864.60	2041.24	2034.05	1981.91	1747.12	1784.60	2071.09	1534.11	1673.14
TAG	TAG45:0-FA14:0	13.55	782.72	537.49	286.47	224.40	397.70	366.39	156.38	150.59	370.05	398.49	413.94	350.44	349.50	304.32	355.66	248.74	324.52
TAG	TAG50:2-FA14:0	13.81	848.80	603.60	62.46	NA	96.42	NA	NA	NA	72.10	NA	78.12	NA	75.51	75.12	NA	64.09	NA
TAG	TAG46:1-FA16:0	13.41	794.70	521.40	267.37	293.65	377.15	322.45	129.79	138.36	326.77	357.25	322.11	322.85	280.80	287.30	293.44	220.70	303.88
TAG	TAG54:7-FA18:2	12.71	894.80	597.50	31.51	37.18	40.33	38.32	16.13	NA	30.04	29.35	32.78	30.09	34.65	NA	42.43	30.62	31.61
TAG	TAG49:3-FA16:1	13.28	832.80	561.50	137.27	120.64	155.86	93.51	58.57	59.95	113.75	103.80	116.26	115.28	106.27	121.57	90.77	113.48	109.16
TAG	TAG51:1-FA17:0	14.38	864.80	577.50	73.21	72.62	144.83	95.74	51.18	35.16	111.32	120.53	125.18	93.74	103.19	92.08	103.72	83.22	90.07
TAG	TAG54:0-FA18:0	15.25	908.80	607.50	1702.46	1290.61	1506.48	2175.83	1356.77	1452.13	1355.64	1507.52	1510.51	781.14	681.03	1391.66	758.86	1189.85	1451.81
TAG	TAG48:2-FA16:1	13.48	820.70	549.40	565.40	556.14	852.66	616.73	328.13	300.91	639.86	720.91	704.39	741.28	567.31	657.85	599.17	515.42	586.74
TAG	TAG49:2-FA16:1	13.67	834.80	563.50	332.00	298.77	477.03	385.30	179.08	178.50	361.88	382.29	409.94	360.68	355.80	374.07	391.33	307.50	348.64
TAG	TAG51:2-FA16:1	14.07	862.80	591.50	96.26	78.46	135.73	99.12	28.93	46.81	86.81	91.41	98.51	102.18	95.51	97.17	111.36	92.81	94.82
TAG	TAG49:2-FA18:1	13.65	834.80	535.50	130.15	121.55	267.64	194.23	73.35	69.06	162.60	159.37	179.92	126.10	166.52	155.25	171.27	108.36	148.28
TAG	TAG48:2-FA18:1	13.44	820.70	521.40	117.73	139.48	184.70	154.48	92.67	87.99	157.93	139.61	155.84	160.58	115.61	152.72	122.38	125.75	154.50
TAG	TAG51:0-FA16:0	14.75	866.80	593.50	103.24	83.45	125.94	138.59	51.65	50.31	108.35	117.08	102.47	118.11	101.12	95.22	108.35	90.49	91.27
TAG	TAG48:1-FA16:0	13.84	822.70	549.40	556.23	563.11	784.30	647.34	300.89	283.12	578.96	661.81	613.42	589.36	496.80	630.79	557.07	500.93	563.71
TAG	TAG47:0-FA17:0	13.95	810.70	523.47	178.94	145.91	281.39	268.03	88.27	72.72	191.55	206.96	219.86	189.67	212.55	173.21	185.05	133.32	167.05
TAG	TAG56:1-FA16:0	15.27	934.90	661.60	49.59	45.40	57.24	59.30	31.13	33.75	55.59	61.58	63.63	63.03	54.95	53.12	60.13	46.35	45.56
TAG	TAG51:0-FA18:0	14.75	866.80	565.50	89.51	79.15	103.13	108.75	52.90	70.46	91.15	97.06	104.82	85.20	79.86	92.33	90.60	59.00	83.12
TAG	TAG49:1-FA16:0	14.02	836.80	563.50	317.64	285.64	416.19	320.19	174.06	176.64	328.14	378.14	360.66	333.89	302.03	311.64	343.73	227.77	306.37
TAG	TAG49:0-FA16:0	14.39	838.80	565.50	386.98	378.78	429.54	566.97	209.69	275.54	454.65	499.16	433.79	531.43	405.12	407.77	500.91	327.76	396.80
TAG	TAG47:2-FA16:1	13.23	806.70	535.40	338.09	338.35	530.77	413.40	176.74	164.88	386.04	395.18	441.31	377.25	399.58	385.80	391.47	350.59	365.64
TAG	TAG44:2-FA16:1	12.43	764.68	493.43	123.87	131.05	198.47	147.00	63.78	70.95	156.57	145.58	168.44	130.39	131.93	141.11	117.45	113.69	136.44
TAG	TAG42:1-FA14:0	12.32	738.66	493.43	38.22	31.86	62.13	42.82	23.76	19.41	39.02	39.06	44.28	38.61	53.95	59.35	40.13	35.49	39.34

Table 1. Continued...

Class	CompoundName	RT	Q1	Q3	C-2016-1-1	C-2016-2-1	C-2016-3-1	C-2016-4-1	C-2016-5-1	C-2016-6-1	QC-01	QC-02	QC-03	Y-2016-1-1	Y-2016-2-1	Y-2016-3-1	Y-2016-4-1	Y-2016-5-1	Y-2016-6-1
TAG	TAG56:1-FA18:1	15.26	934.90	635.60	29.94	27.12	47.65	41.99	24.45	NA	34.24	39.52	35.25	40.37	32.63	35.76	39.14	29.87	25.55
TAG	TAG53:0-FA16:0	15.10	894.80	621.50	48.33	46.57	54.35	55.07	32.32	29.89	53.15	57.51	49.20	59.14	48.05	51.19	51.33	37.07	43.77
TAG	TAG46:0-FA14:0	13.79	796.70	551.50	375.38	361.03	483.47	596.52	235.22	215.14	433.64	507.83	458.87	380.40	376.43	339.14	466.37	323.11	373.94
TAG	TAG52:4-FA16:0	13.49	872.80	599.50	NA	216.46	281.84	252.76	NA	NA	197.26	188.06	220.07	242.41	208.73	211.80	241.03	204.21	196.79
TAG	TAG47:0-FA16:0	14.00	810.70	537.40	585.75	615.38	884.36	1002.78	356.94	377.22	762.79	876.11	890.41	851.36	766.15	731.81	917.94	562.51	713.05
TAG	TAG54:5-FA18:2	13.50	898.80	601.50	386.38	NA	NA	NA	NA	NA	359.73	NA	404.83	452.71	NA	NA	419.06	NA	374.78
TAG	TAG48:1-FA14:0	13.81	822.70	577.50	184.77	129.25	259.72	158.23	89.26	NA	184.32	217.57	196.97	168.55	200.91	208.57	142.14	160.82	159.66
TAG	TAG52:0-FA20:0	14.94	880.80	551.50	38.21	33.42	35.33	64.56	24.88	26.63	40.19	44.35	47.75	42.70	41.82	39.96	38.80	30.87	45.37
TAG	TAG52:0-FA16:0	14.93	880.80	607.50	950.01	897.69	945.81	1926.09	751.05	872.98	906.89	1077.19	1030.28	718.62	693.44	1020.64	796.84	872.67	964.15
TAG	TAG49:1-FA16:1	14.02	836.80	565.50	252.88	203.77	367.54	277.17	113.22	119.89	257.92	279.86	309.17	306.46	298.36	280.02	266.10	196.71	268.29
TAG	TAG54:1-FA18:0	14.93	906.80	605.50	142.32	NA	482.74	168.40	NA	NA	213.05	254.36	225.03	261.46	241.28	192.83	267.40	182.26	159.65
TAG	TAG51:1-FA16:0	14.39	864.80	591.50	87.68	108.42	137.83	90.49	60.43	64.84	109.79	128.29	130.37	102.91	113.29	108.89	112.46	101.93	101.53
TAG	TAG54:1-FA18:1	14.93	906.80	607.50	NA	NA	180.79	NA	NA	NA	87.25	94.67	105.06	110.06	96.46	89.23	120.59	NA	NA
TAG	TAG44:2-FA14:0	12.43	764.68	519.44	25.05	18.52	35.64	38.92	12.93	NA	30.02	36.47	34.47	22.97	21.31	22.54	15.92	19.66	21.24
TAG	TAG48:1-FA18:1	13.80	822.70	523.47	256.05	196.64	341.03	292.20	149.96	122.59	241.88	287.09	289.38	276.42	284.20	248.15	271.51	251.48	212.91
TAG	TAG46:1-FA16:1	13.36	794.70	495.44	134.13	100.26	120.46	94.03	63.07	59.73	110.30	117.53	133.55	98.91	127.17	104.65	89.30	102.12	82.93
TAG	TAG52:4-FA18:2	13.49	872.80	575.50	292.14	226.62	310.15	253.91	NA	NA	240.39	264.96	293.45	303.82	294.85	238.44	304.57	261.27	298.28
TAG	TAG54:6-FA18:2	13.11	896.80	599.50	274.50	264.34	338.80	294.13	197.85	175.73	270.10	319.80	326.08	375.58	266.14	279.12	326.03	239.81	348.67
TAG	TAG50:2-FA18:1	13.84	848.80	549.50	383.01	313.10	433.10	346.14	NA	156.37	316.31	363.15	388.89	384.42	482.77	314.99	360.38	288.89	358.91
TAG	TAG49:0-FA17:0	14.38	838.80	551.50	186.74	209.66	373.51	314.98	156.11	150.31	259.18	314.44	269.39	267.56	260.81	236.81	295.12	176.28	227.01
TAG	TAG51:2-FA17:0	14.05	862.80	575.50	25.36	43.97	65.41	34.60	22.24	26.05	60.24	63.92	51.82	62.91	50.29	32.66	37.21	28.02	40.12
TAG	TAG48:0-FA18:0	14.21	824.70	523.47	110.26	94.52	131.97	194.95	81.90	68.14	127.36	143.84	116.27	115.04	125.55	102.74	132.86	97.69	126.26
TAG	TAG44:0-FA14:0	13.33	768.71	523.47	311.02	317.58	377.65	394.61	176.24	177.26	409.31	352.78	437.40	384.25	347.34	393.88	376.79	260.52	328.67
TAG	TAG50:2-FA16:1	13.88	848.80	577.50	373.04	356.59	469.86	436.26	256.23	NA	473.79	580.66	495.60	452.43	543.25	412.53	422.24	380.18	380.59
TAG	TAG46:2-FA14:0	13.00	792.70	547.50	68.63	85.55	102.46	98.10	36.73	37.34	82.96	101.99	87.54	96.59	102.30	78.01	58.58	61.23	100.42
TAG	TAG48:3-FA16:1	13.08	818.70	547.40	192.19	180.92	319.65	260.98	77.72	90.92	212.94	265.53	242.43	230.56	257.49	237.05	274.44	178.94	211.36
TAG	TAG46:1-FA14:0	13.39	794.70	549.50	211.51	191.95	290.56	268.78	140.48	156.37	261.81	293.12	326.54	175.92	263.67	254.45	255.29	258.01	259.24
TAG	TAG47:1-FA16:1	13.62	808.70	537.40	465.08	474.59	643.51	541.67	218.62	273.45	527.68	604.61	482.66	556.79	480.90	446.84	418.05	410.52	526.74
TAG	TAG44:0-FA16:0	13.34	768.71	495.44	292.85	270.53	351.47	409.83	203.19	192.63	315.27	396.83	366.07	366.03	343.85	289.99	313.56	204.98	327.21
TAG	TAG50:3-FA16:1	13.49	846.80	521.40	271.38	218.37	345.08	250.81	NA	141.20	260.66	327.11	312.83	405.24	432.04	288.04	260.99	215.04	259.74
TAG	TAG44:1-FA18:1	12.86	766.69	467.41	34.13	29.71	NA	NA	NA	NA	24.36	30.67	26.76	NA	46.70	35.04	23.32	31.28	NA
TAG	TAG46:1-FA16:1	13.40	794.70	523.47	439.95	503.45	821.98	623.15	243.29	246.07	547.52	675.46	561.34	465.86	600.86	557.38	575.81	510.72	534.80
TAG	TAG51:1-FA18:1	14.38	864.80	565.50	100.90	116.89	142.21	128.68	61.52	70.69	123.19	140.99	156.30	118.95	128.88	127.11	144.13	103.79	99.26
TAG	TAG44:1-FA16:0	12.90	766.69	493.43	62.52	46.52	93.85	82.95	27.42	32.65	77.98	63.03	64.95	67.34	85.10	87.18	40.19	56.59	67.81
TAG	TAG45:1-FA16:0	13.13	780.71	507.40	56.98	97.75	137.83	73.41	38.08	48.01	112.13	131.32	103.47	81.75	82.39	101.04	90.46	58.81	114.35
TAG	TAG47:1-FA16:0	13.62	808.70	535.40	229.43	248.94	432.22	322.53	136.97	149.83	295.60	367.16	374.04	357.28	365.19	323.76	250.65	254.49	298.62
TAG	TAG49:1-FA18:1	14.00	836.80	537.50	232.53	198.41	343.94	270.27	119.03	154.01	251.11	319.89	270.20	256.92	286.00	242.04	215.68	194.23	243.78
TAG	TAG46:2-FA16:1	12.99	792.70	521.40	349.95	297.70	510.39	400.16	187.77	169.31	341.19	435.38	426.91	371.12	375.59	385.59	396.08	244.83	344.25
TAG	TAG52:2-FA18:2	14.26	876.80	579.50	120.39	60.27	90.97	69.26	NA	58.92	70.54	72.32	89.26	98.76	69.64	84.26	124.39	NA	82.44

Table 1. Continued...

Class	CompoundName	RT	Q1	Q3	C-2016-1-1	C-2016-2-1	C-2016-3-1	C-2016-4-1	C-2016-5-1	C-2016-6-1	QC-01	QC-02	QC-03	Y-2016-1-1	Y-2016-2-1	Y-2016-3-1	Y-2016-4-1	Y-2016-5-1	Y-2016-6-1
TAG	TAG48:2-FA16:0	13.47	820.70	547.40	126.80	110.06	188.46	172.46	75.26	60.35	134.87	165.12	175.73	138.90	184.58	136.14	150.82	159.92	163.07
TAG	TAG49:2-FA18:2	13.71	834.80	537.50	57.12	71.09	68.98	74.14	49.41	22.13	71.12	87.01	93.78	82.13	53.42	73.91	72.48	71.82	79.08
TAG	TAG50:3-FA14:0	13.43	846.80	601.60	NA	22.16	18.10	NA	NA	NA	32.36	NA	26.56	NA	18.76	NA	25.75	23.06	20.47
TAG	TAG47:1-FA18:1	13.56	808.70	509.40	117.59	105.81	150.50	89.10	50.95	63.11	104.79	139.05	127.54	137.31	107.04	129.56	116.98	71.60	118.04
TAG	TAG52:1-FA16:1	14.63	878.80	607.50	52.56	47.02	87.39	57.95	29.40	25.02	63.60	54.70	72.73	59.69	65.22	71.15	41.76	37.05	46.18
TAG	TAG53:2-FA18:1	14.40	890.80	591.50	75.44	NA	70.66	77.02	NA	NA	79.84	81.40	62.06	69.57	NA	64.39	75.44	66.67	72.70
TAG	TAG49:1-FA17:0	14.01	836.80	549.50	150.79	97.35	214.07	140.35	46.76	73.25	121.06	159.86	131.77	162.42	144.05	93.53	154.71	118.57	127.87
TAG	TAG51:2-FA18:1	14.04	862.80	563.50	151.29	150.50	199.32	145.39	86.84	96.14	140.36	185.69	187.37	161.54	169.16	148.04	145.62	141.41	143.00
TAG	TAG54:1-FA16:0	14.94	906.80	633.50	36.68	34.95	53.77	47.59	NA	NA	40.60	55.24	52.97	45.04	43.50	40.99	52.79	37.60	38.07
TAG	TAG52:4-FA16:1	13.48	872.80	601.50	NA	NA	NA	NA	NA	NA	58.36	46.39	NA	NA	78.89	61.30	70.10	NA	58.48
TAG	TAG49:2-FA16:0	13.67	834.80	561.50	88.85	64.46	151.81	82.45	46.62	49.17	100.68	138.00	113.13	83.68	79.16	81.93	78.56	59.99	89.55
TAG	TAG46:3-FA16:1	12.55	790.70	519.44	60.27	91.11	143.68	119.50	47.06	45.77	86.74	110.39	120.30	96.73	99.70	98.94	72.34	57.88	77.83
TAG	TAG48:0-FA14:0	14.21	824.70	579.50	86.35	94.21	100.96	157.28	60.98	44.95	136.84	98.17	125.54	120.42	76.75	81.84	115.29	54.60	76.99
TAG	TAG42:1-FA16:1	12.31	738.66	467.41	49.51	37.79	75.44	49.13	18.25	20.78	51.28	42.56	60.32	38.53	50.35	31.77	47.04	40.03	43.32
TAG	TAG50:3-FA18:1	13.48	846.80	547.50	91.94	93.23	128.46	69.44	44.34	62.13	97.53	118.36	140.48	156.38	157.82	106.08	97.10	91.49	85.22
TAG	TAG44:1-FA16:1	12.89	766.69	495.44	192.23	187.79	289.52	208.66	110.52	108.27	187.08	272.77	258.55	176.30	189.33	199.96	178.69	169.23	213.14
TAG	TAG56:4-FA18:2	14.26	928.80	631.50	26.63	NA	39.74	24.09	NA	NA	19.93	25.15	29.54	NA	18.04	19.28	24.75	26.03	NA
TAG	TAG51:3-FA18:2	13.73	860.80	563.50	35.32	32.57	87.85	41.93	26.30	20.31	62.20	47.32	71.13	43.33	34.93	52.25	43.31	42.66	39.45
TAG	TAG50:1-FA16:1	14.26	850.80	579.50	128.92	129.00	154.91	106.95	50.38	52.85	105.08	157.13	125.78	156.88	144.12	117.95	113.65	86.90	113.59
TAG	TAG50:3-FA18:2	13.51	846.80	565.50	70.36	76.74	130.49	108.98	NA	51.67	102.15	125.06	153.51	122.25	97.96	99.50	118.90	95.35	115.18
TAG	TAG42:0-FA14:0	12.81	740.68	495.44	109.64	65.88	120.62	142.19	60.84	65.21	99.92	117.54	150.17	105.24	66.40	104.94	120.25	62.53	89.93
TAG	TAG47:2-FA18:1	13.19	806.70	507.40	36.74	54.44	50.30	22.39	25.61	31.94	38.92	55.39	39.09	34.62	29.74	56.44	49.13	35.97	37.41
TAG	TAG54:4-FA18:0	13.93	900.80	599.50	61.14	55.46	91.80	55.84	52.82	51.98	48.38	50.51	70.49	NA	73.64	73.57	67.68	67.22	80.97
TAG	TAG48:2-FA18:2	13.44	820.70	523.47	29.94	20.94	28.03	27.14	NA	NA	31.23	25.72	39.73	NA	21.33	36.45	56.92	80.69	102.08
TAG	TAG47:0-FA14:0	13.97	810.70	565.50	131.76	110.68	169.11	185.59	98.10	60.91	129.28	145.64	198.37	139.81	178.66	166.47	148.83	104.38	137.77
TAG	TAG50:0-FA14:0	14.59	852.80	607.60	50.34	43.53	48.45	76.37	33.47	26.69	46.15	41.76	63.91	58.90	41.21	43.34	51.45	30.02	48.42
TAG	TAG51:2-FA16:0	14.06	862.80	589.50	53.63	37.04	59.62	36.44	32.66	44.63	63.28	45.85	41.17	48.68	39.14	53.49	65.18	39.91	37.40
TAG	TAG48:2-FA14:0	13.42	820.70	575.50	72.00	75.96	91.80	89.18	51.37	NA	69.32	110.70	102.97	79.53	88.27	101.50	72.19	60.71	77.34
TAG	TAG46:0-FA18:0	13.82	796.70	495.44	49.30	31.45	57.71	36.61	24.13	NA	46.70	40.83	63.80	41.73	64.97	41.13	63.09	35.00	43.22
TAG	TAG52:2-FA16:1	14.26	876.80	605.50	89.27	61.65	98.10	69.11	12.95	16.09	127.96	101.14	77.93	171.31	208.60	137.51	61.55	74.19	75.89
TAG	TAG50:1-FA14:0	14.40	864.80	563.50	27.56	35.01	31.62	31.91	18.83	20.35	37.43	59.53	42.39	33.09	47.53	37.42	41.16	31.25	33.31
TAG	TAG51:1-FA18:0	13.66	834.80	547.50	40.45	43.17	61.78	74.69	12.95	16.09	55.30	69.07	41.34	49.50	47.67	36.24	56.70	38.70	48.63
TAG	TAG49:2-FA17:0	14.63	904.80	607.50	20.19	29.65	29.04	25.73	15.91	17.03	21.37	37.18	32.86	37.39	30.10	33.75	34.35	29.76	22.31
TAG	TAG47:2-FA14:0	13.20	806.70	561.50	28.40	36.68	39.08	41.54	NA	24.98	36.84	48.42	28.30	21.81	37.13	32.68	47.84	40.09	18.61
TAG	TAG50:1-FA18:0	14.23	850.80	549.50	89.79	82.15	121.40	90.40	51.37	42.23	87.04	92.09	138.30	130.35	100.51	79.90	100.40	88.79	78.30
TAG	TAG54:2-FA18:2	14.63	904.80	607.50	34.35	29.65	29.04	25.73	15.91	17.03	21.37	37.18	32.86	37.39	30.10	33.75	34.35	29.76	22.31
TAG	TAG48:1-FA18:0	13.84	822.70	521.40	31.80	25.39	60.96	47.72	17.99	NA	55.06	32.00	41.33	35.41	37.79	38.14	48.72	42.86	29.53
TAG	TAG42:0-FA16:0	12.83	740.676	467.409	57.35817435	41.65432279	NA	102.5235262	56.95218884	NA	55.25950267	86.92682918	52.22604436	87.56578552	70.7018965	63.85722505	45.97131621	NA	81.3628296

Table 2. Difference analysis of Lipids molecular species in icewine samples.

id	MS2 name	Lipid species	P-VALUE	Relative difference (%)
1	Cer(18:1/26:1)	Cer	0.517275692	-12.27229618
2	Cer(18:1/26:0)	Cer	0.514515615	-13.61275079
3	Cer(18:1/22:0)	Cer	0.911780234	-2.668059765
4	Cer(18:1/24:0)	Cer	0.894389304	3.38906541
5	Cer(18:1/16:1)	Cer	0.304462824	-28.40333742
6	Cer(18:1/24:1)	Cer	0.787299618	6.647632834
7	DAG(16:0/16:1)	DAG	0.9855332	-0.591800657
8	DAG(16:0/16:0)	DAG	0.065607899	105.0663258
9	DAG(14:0/20:0)	DAG	0.025398555	75.8946734
10	DAG(16:0/18:0)	DAG	0.069899821	103.1598151
11	DAG(16:1/16:1)	DAG	0.843944783	5.215116719
12	FFA(24:6)	FFA	0.007291779	-54.47161154
13	FFA(18:0)	FFA	0.282744787	-29.32675629
14	FFA(18:3)	FFA	0.001759833	-46.92448768
15	FFA(20:0)	FFA	0.02059842	-50.59648202
16	FFA(14:0)	FFA	0.326256221	-24.37942387
17	FFA(18:1)	FFA	0.00418488	-45.31093068
18	FFA(16:0)	FFA	0.813077729	8.083868768
19	FFA(22:1)	FFA	0.166281119	-37.43762485
20	FFA(16:1)	FFA	0.927049381	-2.297788193
21	FFA(24:0)	FFA	0.032609547	38678.00366
22	FFA(20:5)	FFA	0.395446297	22.68620317
23	FFA(28:0)	FFA	0.066080336	-45.71258269
24	FFA(18:2)	FFA	0.00158313	-42.43984332
25	FFA(20:4)	FFA	0.006690701	-47.70371316
26	FFA(20:1)	FFA	0.820146885	-7.444209228
27	FFA(22:0)	FFA	0.039511188	-44.11424925
28	FFA(20:2)	FFA	0.243296792	-31.57398633
29	FFA(26:0)	FFA	0.45401809	92.41421279
30	SM(14:0)	SM	0.497844395	7.326085751
31	TAG(50:0)_FA18:0	TAG	0.18662233	-24.49513983
32	TAG(51:0)_FA17:0	TAG	0.609042715	-9.28315591
33	TAG(47:1)_FA17:0	TAG	0.820523486	4.69201044
34	TAG(49:0)_FA18:0	TAG	0.806502797	-4.336003994
35	TAG(52:0)_FA18:0	TAG	0.81812297	-4.893973844
36	TAG(48:1)_FA16:1	TAG	0.203533918	-32.51649383
37	TAG(44:0)_FA18:0	TAG	0.245313307	-42.09748476
38	TAG(44:1)_FA14:0	TAG	0.13220125	-24.34726925
39	TAG(46:0)_FA16:0	TAG	0.217757218	-25.99113212
40	TAG(47:1)_FA14:0	TAG	0.218760146	-17.30783962
41	TAG(45:0)_FA16:0	TAG	0.397833765	-11.66276117
42	TAG(50:0)_FA16:0	TAG	0.156790918	-25.6253194
43	TAG(54:0)_FA16:0	TAG	0.740349579	4.539929383
44	TAG(48:0)_FA16:0	TAG	0.121439397	-29.33441363
45	TAG(45:0)_FA14:0	TAG	0.231172093	-18.16947068
46	TAG(50:2)_FA14:0	TAG	0.21405187	-68.02404488
47	TAG(46:1)_FA16:0	TAG	0.329009014	-26.05625687

Table 2. Continued...

id	MS2 name	Lipid species	P-VALUE	Relative difference (%)
48	TAG(54:7)_FA18:2	TAG	0.72514185	-11.99893768
49	TAG(49:3)_FA16:1	TAG	0.774789674	-4.68149988
50	TAG(51:1)_FA17:0	TAG	0.038009743	-47.73563692
51	TAG(54:0)_FA18:0	TAG	0.553269558	16.87854383
52	TAG(48:2)_FA16:1	TAG	0.055810228	-52.48115511
53	TAG(49:2)_FA16:1	TAG	0.251583927	-30.02065344
54	TAG(51:2)_FA16:1	TAG	0.048414341	-53.11245492
55	TAG(49:2)_FA18:1	TAG	0.144159061	-32.64760999
56	TAG(48:2)_FA18:1	TAG	0.608986263	-6.555639127
57	TAG(51:0)_FA16:0	TAG	0.361406507	-24.85529714
58	TAG(48:1)_FA16:0	TAG	0.105266254	-46.94645531
59	TAG(47:0)_FA17:0	TAG	0.245653402	-28.79214704
60	TAG(56:1)_FA16:0	TAG	0.193990793	-14.45708953
61	TAG(51:0)_FA18:0	TAG	0.719626805	-7.665981201
62	TAG(49:1)_FA16:0	TAG	0.08207137	-49.15847376
63	TAG(49:0)_FA16:0	TAG	0.315436646	-20.64153139
64	TAG(47:2)_FA16:1	TAG	0.061560096	-51.79387477
65	TAG(44:2)_FA16:1	TAG	0.097177331	-47.27405413
66	TAG(42:1)_FA14:0	TAG	0.031127561	-40.94441607
67	TAG(56:1)_FA18:1	TAG	0.490411645	-15.06473627
68	TAG(53:0)_FA16:0	TAG	0.474600622	-8.267247148
69	TAG(46:0)_FA14:0	TAG	0.172039042	-35.46189636
70	TAG(52:4)_FA16:0	TAG	0.165902946	-42.0928616
71	TAG(47:0)_FA16:0	TAG	0.333763155	-15.85754826
72	TAG(54:5)_FA18:2	TAG	0.235118398	-68.504602
73	TAG(48:1)_FA14:0	TAG	0.056199352	-45.74723225
74	TAG(52:0)_FA20:0	TAG	0.060194888	-33.20114457
75	TAG(52:0)_FA16:0	TAG	0.522510034	-12.77592439
76	TAG(49:1)_FA16:1	TAG	0.300544305	-17.41857571
77	TAG(54:1)_FA18:0	TAG	0.001341041	-75.71781098
78	TAG(51:1)_FA16:0	TAG	0.254548513	-14.24748048
79	TAG(54:1)_FA18:1	TAG	0.026910236	-97.80499079
80	TAG(44:2)_FA14:0	TAG	0.054472166	-50.57113678
81	TAG(48:1)_FA18:1	TAG	0.424092515	-12.05495563
82	TAG(46:1)_FA18:1	TAG	0.693270843	-5.519473354
83	TAG(52:4)_FA18:2	TAG	0.138832803	-36.17107523
84	TAG(54:6)_FA18:2	TAG	0.171443798	-15.800566
85	TAG(50:2)_FA18:1	TAG	0.703993992	-13.49884813
86	TAG(49:0)_FA17:0	TAG	0.774533037	-4.938892696
87	TAG(51:2)_FA17:0	TAG	0.523200632	-13.36596665
88	TAG(48:0)_FA18:0	TAG	0.116486884	-30.25281852
89	TAG(44:0)_FA14:0	TAG	0.231740231	-24.47112254
90	TAG(50:2)_FA16:1	TAG	0.133366339	-36.75461725
91	TAG(46:2)_FA14:0	TAG	0.446746628	-13.7450348
92	TAG(48:3)_FA16:1	TAG	0.315147678	-19.24491359
93	TAG(46:1)_FA14:0	TAG	0.247653005	-14.1090195
94	TAG(47:1)_FA16:1	TAG	0.479336783	-15.49423569
95	TAG(44:0)_FA16:0	TAG	0.625525495	-6.779576281

Table 2. Continued...

id	MS2 name	Lipid species	P-VALUE	Relative difference (%)
96	TAG(50:3)_FA16:1	TAG	0.1124473	-33.9973152
97	TAG(44:1)_FA18:1	TAG	0.668421336	-25.7369757
98	TAG(46:1)_FA16:1	TAG	0.065703762	-51.58863615
99	TAG(51:1)_FA18:1	TAG	0.280598465	-14.01719475
100	TAG(44:1)_FA16:0	TAG	0.477380178	-14.42317162
101	TAG(45:1)_FA16:0	TAG	0.469352183	-14.51166095
102	TAG(47:1)_FA16:0	TAG	0.293394496	-17.84152909
103	TAG(49:1)_FA18:1	TAG	0.585974968	-8.372126492
104	TAG(46:2)_FA16:1	TAG	0.572011438	-9.547973329
105	TAG(52:2)_FA18:2	TAG	0.679330051	-12.94511099
106	TAG(48:2)_FA16:0	TAG	0.18129076	-21.43058143
107	TAG(49:2)_FA18:2	TAG	0.168101662	-25.54491217
108	TAG(50:3)_FA14:0	TAG	0.237795573	-49.07056222
109	TAG(47:1)_FA18:1	TAG	0.351630799	-15.20383615
110	TAG(52:1)_FA16:1	TAG	0.74353992	-6.764752893
111	TAG(53:2)_FA18:1	TAG	0.329923721	-34.99111563
112	TAG(49:1)_FA17:0	TAG	0.635403214	-9.808577912
113	TAG(51:2)_FA18:1	TAG	0.069025861	-50.28733366
114	TAG(54:1)_FA16:0	TAG	0.204800684	-31.75619862
115	TAG(49:2)_FA16:0	TAG	0.134670714	-29.56144399
116	TAG(46:3)_FA16:1	TAG	0.971441786	0.788545323
117	TAG(48:0)_FA14:0	TAG	0.24517369	-26.03127902
118	TAG(42:1)_FA16:1	TAG	0.185389705	-29.49594912
119	TAG(50:3)_FA18:1	TAG	0.741895791	-8.971605122
120	TAG(44:1)_FA16:1	TAG	0.09757849	-47.34092806
121	TAG(56:4)_FA18:2	TAG	0.416708343	-37.63412505
122	TAG(51:3)_FA18:2	TAG	0.041058439	-45.61524281
123	TAG(50:1)_FA16:1	TAG	0.278713113	-28.67923736
124	TAG(50:3)_FA18:2	TAG	0.119410729	-32.25213343
125	TAG(42:0)_FA14:0	TAG	0.885235886	2.748325624
126	TAG(47:2)_FA18:1	TAG	0.599625591	-8.995308132
127	TAG(54:4)_FA18:0	TAG	0.364655588	-23.54464134
128	TAG(48:2)_FA18:2	TAG	0.311547383	-45.00883968
129	TAG(47:0)_FA14:0	TAG	0.377649632	-13.67282538
130	TAG(50:0)_FA14:0	TAG	0.203240527	-25.36290583
131	TAG(51:2)_FA16:0	TAG	0.605955494	-6.972099996
132	TAG(48:2)_FA14:0	TAG	0.29964312	-20.37191611
133	TAG(46:0)_FA18:0	TAG	0.155078595	-30.57466762
134	TAG(52:2)_FA16:1	TAG	0.047627058	-55.94186451
135	TAG(50:1)_FA14:0	TAG	0.370487433	-27.33850526
136	TAG(51:1)_FA18:0	TAG	0.111969048	-45.93547537
137	TAG(49:2)_FA17:0	TAG	0.458332974	-16.82488238
138	TAG(47:2)_FA14:0	TAG	0.579157953	-13.09653686
139	TAG(50:1)_FA18:0	TAG	0.234252279	-24.48921714
140	TAG(54:2)_FA18:2	TAG	0.028341716	-26.69845708
141	TAG(48:1)_FA18:0	TAG	0.420205034	-20.23833182
142	TAG(42:0)_FA16:0	TAG	0.479060441	-25.48096807

Table 3. TAG lipids molecular species and content in icewine samples.

id	MS2 name	C-2016	Y-2016	VIP	P-VALUE	Q-VALUE
1	TAG(50:0)_FA18:0	14.73	19.52	0.87	0.19	0.25
2	TAG(51:0)_FA17:0	1.26	1.39	0.61	0.61	0.39
3	TAG(47:1)_FA17:0	1.22	1.17	0.11	0.82	0.47
4	TAG(49:0)_FA18:0	2.22	2.32	0.53	0.81	0.46
5	TAG(52:0)_FA18:0	32.27	33.93	0.73	0.82	0.47
6	TAG(48:1)_FA16:1	7.14	10.59	1.11	0.2	0.26
7	TAG(44:0)_FA18:0	0.33	0.58	1.03	0.25	0.26
8	TAG(44:1)_FA14:0	2.18	2.88	1.04	0.13	0.23
9	TAG(46:0)_FA16:0	11.23	15.18	0.94	0.22	0.26
10	TAG(47:1)_FA14:0	2.08	2.52	0.59	0.22	0.26
11	TAG(45:0)_FA16:0	7.27	8.23	0.61	0.4	0.32
12	TAG(50:0)_FA16:0	26.75	35.96	0.88	0.16	0.24
13	TAG(54:0)_FA16:0	1.76	1.69	0.02	0.74	0.44
14	TAG(48:0)_FA16:0	25.42	35.97	0.92	0.12	0.23
15	TAG(45:0)_FA14:0	5.27	6.44	0.86	0.23	0.26
16	TAG(50:2)_FA14:0	0.23	0.73	1.06	0.21	0.26
17	TAG(46:1)_FA16:0	4.21	5.7	1.08	0.33	0.29
18	TAG(54:7)_FA18:2	0.5	0.57	0.64	0.73	0.44
19	TAG(49:3)_FA16:1	2.09	2.19	0.57	0.77	0.45
20	TAG(51:1)_FA17:0	0.99	1.89	1.5	0.04	0.17
21	TAG(54:0)_FA18:0	24.37	20.85	0.59	0.55	0.37
22	TAG(48:2)_FA16:1	5.81	12.23	1.59	0.06	0.18
23	TAG(49:2)_FA16:1	4.99	7.13	1.1	0.25	0.27
24	TAG(51:2)_FA16:1	0.93	1.98	1.62	0.05	0.18
25	TAG(49:2)_FA18:1	1.97	2.92	1.17	0.14	0.24
26	TAG(48:2)_FA18:1	2.59	2.77	0.2	0.61	0.39
27	TAG(51:0)_FA16:0	1.51	2.02	1.06	0.36	0.3
28	TAG(48:1)_FA16:0	5.9	11.13	1.57	0.11	0.22
29	TAG(47:0)_FA17:0	2.52	3.54	1.15	0.25	0.26
30	TAG(56:1)_FA16:0	0.92	1.08	0.96	0.19	0.25
31	TAG(51:0)_FA18:0	1.51	1.63	0.53	0.72	0.43
32	TAG(49:1)_FA16:0	3.09	6.08	1.59	0.08	0.2
33	TAG(49:0)_FA16:0	6.8	8.57	0.67	0.32	0.29
34	TAG(47:2)_FA16:1	3.65	7.57	1.6	0.06	0.19
35	TAG(44:2)_FA16:1	1.36	2.57	1.56	0.1	0.21
36	TAG(42:1)_FA14:0	0.53	0.89	1.33	0.03	0.16
37	TAG(56:1)_FA18:1	0.58	0.68	0.83	0.49	0.35
38	TAG(53:0)_FA16:0	0.89	0.97	0.64	0.47	0.34
39	TAG(46:0)_FA14:0	4.86	7.53	1.31	0.17	0.25
40	TAG(52:4)_FA16:0	2.52	4.35	1.03	0.17	0.25
41	TAG(47:0)_FA16:0	12.74	15.14	0.74	0.33	0.29
42	TAG(54:5)_FA18:2	1.31	4.17	0.95	0.24	0.26
43	TAG(48:1)_FA14:0	1.88	3.47	1.48	0.06	0.18
44	TAG(52:0)_FA20:0	0.53	0.8	1.08	0.06	0.19
45	TAG(52:0)_FA16:0	14.73	16.89	0.78	0.52	0.36
46	TAG(49:1)_FA16:1	4.45	5.39	0.81	0.3	0.28
47	TAG(54:1)_FA18:0	1.06	4.35	1.67	0	0.04
48	TAG(51:1)_FA16:0	1.83	2.14	0.96	0.25	0.27
49	TAG(54:1)_FA18:1	0.03	1.4	1.64	0.03	0.16
50	TAG(44:2)_FA14:0	0.2	0.41	1.77	0.05	0.18
51	TAG(48:1)_FA18:1	4.53	5.15	0.78	0.42	0.33
52	TAG(46:1)_FA18:1	1.91	2.02	0.78	0.69	0.42
53	TAG(52:4)_FA18:2	3.62	5.67	1.16	0.14	0.24
54	TAG(54:6)_FA18:2	5.15	6.12	0.85	0.17	0.25
55	TAG(50:2)_FA18:1	4.93	5.7	0.39	0.7	0.43
56	TAG(49:0)_FA17:0	4.64	4.88	0.24	0.77	0.45

Table 3. Continued...

id	MS2 name	C-2016	Y-2016	VIP	P-VALUE	Q-VALUE
57	TAG(51:2)_FA17:0	0.73	0.84	0.45	0.52	0.36
58	TAG(48:0)_FA18:0	1.63	2.33	1	0.12	0.23
59	TAG(44:0)_FA14:0	5.27	6.97	0.72	0.23	0.26
60	TAG(50:2)_FA16:1	5.46	8.64	1.16	0.13	0.23
61	TAG(46:2)_FA14:0	1.43	1.66	0.57	0.45	0.33
62	TAG(48:3)_FA16:1	3.74	4.63	0.87	0.32	0.29
63	TAG(46:1)_FA14:0	4.2	4.89	0.71	0.25	0.26
64	TAG(47:1)_FA16:1	8	9.47	0.63	0.48	0.34
65	TAG(44:0)_FA16:0	5.73	6.15	0.38	0.63	0.4
66	TAG(50:3)_FA16:1	4.09	6.2	0.81	0.11	0.22
67	TAG(44:1)_FA18:1	0.23	0.31	0.85	0.67	0.42
68	TAG(46:1)_FA16:1	5.24	10.82	1.59	0.07	0.19
69	TAG(51:1)_FA18:1	2.07	2.41	0.9	0.28	0.28
70	TAG(44:1)_FA16:0	1.15	1.35	0.42	0.48	0.34
71	TAG(45:1)_FA16:0	1.51	1.76	0.52	0.47	0.34
72	TAG(47:1)_FA16:0	5.07	6.17	0.71	0.29	0.28
73	TAG(49:1)_FA18:1	4.39	4.8	0.44	0.59	0.38
74	TAG(46:2)_FA16:1	6.38	7.06	0.58	0.57	0.38
75	TAG(52:2)_FA18:2	1.34	1.54	0.16	0.68	0.42
76	TAG(48:2)_FA16:0	2.44	3.11	0.97	0.18	0.25
77	TAG(49:2)_FA18:2	1.07	1.44	0.95	0.17	0.25
78	TAG(50:3)_FA14:0	0.15	0.3	0.89	0.24	0.26
79	TAG(47:1)_FA18:1	1.92	2.27	0.75	0.35	0.3
80	TAG(52:1)_FA16:1	1	1.07	0.36	0.74	0.44
81	TAG(53:2)_FA18:1	0.76	1.17	0.5	0.33	0.29
82	TAG(49:1)_FA17:0	2.41	2.67	0.59	0.64	0.4
83	TAG(51:2)_FA18:1	1.51	3.03	1.6	0.07	0.19
84	TAG(54:1)_FA16:0	0.59	0.86	1.11	0.2	0.26
85	TAG(49:2)_FA16:0	1.11	1.58	1.13	0.13	0.23
86	TAG(46:3)_FA16:1	1.69	1.68	0.06	0.97	0.51
87	TAG(48:0)_FA14:0	1.3	1.75	0.98	0.25	0.26
88	TAG(42:1)_FA16:1	0.59	0.84	1.26	0.19	0.25
89	TAG(50:3)_FA18:1	1.63	1.79	0.6	0.74	0.44
90	TAG(44:1)_FA16:1	1.98	3.76	1.57	0.1	0.21
91	TAG(56:4)_FA18:2	0.19	0.3	0.98	0.42	0.32
92	TAG(51:3)_FA18:2	0.46	0.85	1.48	0.04	0.17
93	TAG(50:1)_FA16:1	1.74	2.44	1.11	0.28	0.27
94	TAG(50:3)_FA18:2	1.47	2.16	0.78	0.12	0.23
95	TAG(42:0)_FA14:0	1.88	1.83	0.14	0.89	0.48
96	TAG(47:2)_FA18:1	0.74	0.81	0.6	0.6	0.39
97	TAG(54:4)_FA18:0	0.93	1.22	0.46	0.36	0.3
98	TAG(48:2)_FA18:2	0.36	0.66	0.6	0.31	0.28
99	TAG(47:0)_FA14:0	2.52	2.92	0.73	0.38	0.31
100	TAG(50:0)_FA14:0	0.68	0.91	0.98	0.2	0.26
101	TAG(51:2)_FA16:0	0.88	0.95	0.45	0.61	0.39
102	TAG(48:2)_FA14:0	1.27	1.6	0.91	0.3	0.28
103	TAG(46:0)_FA18:0	0.67	0.96	1.11	0.16	0.24
104	TAG(52:2)_FA16:1	1.07	2.43	1.27	0.05	0.18
105	TAG(50:1)_FA14:0	0.43	0.59	0.48	0.37	0.31
106	TAG(51:1)_FA18:0	0.5	0.92	1.47	0.11	0.22
107	TAG(49:2)_FA17:0	0.68	0.82	0.61	0.46	0.34
108	TAG(47:2)_FA14:0	0.57	0.66	0.63	0.58	0.38
109	TAG(50:1)_FA18:0	1.46	1.93	0.98	0.23	0.26
110	TAG(54:2)_FA18:2	0.46	0.63	1.39	0.03	0.16
111	TAG(48:1)_FA18:0	0.62	0.77	0.91	0.42	0.32
112	TAG(42:0)_FA16:0	0.87	1.17	0.77	0.48	0.34
113	Total	398.26	522.43			

Table 4. FFA lipids molecular species and content in icewine samples.

id	MS2 name	C-2016	Y-2016	VIP	P-VALUE	Q-VALUE
1	FFA(24:6)	1.21	0.6	1.16	0.01	0.09
2	FFA(18:0)	2551.46	356	0.74	0.28	0.28
3	FFA(18:3)	3.05	0.59	1.86	0	0.04
4	FFA(20:0)	39.13	9.19	1.75	0.02	0.14
5	FFA(14:0)	61.24	15.34	0.71	0.33	0.29
6	FFA(18:1)	111.26	25.78	1.81	0	0.07
7	FFA(16:0)	1668.72	251.58	1.27	0.81	0.46
8	FFA(22:1)	31.37	10.01	0.51	0.17	0.25
9	FFA(16:1)	27.59	8.12	0.49	0.93	0.5
10	FFA(24:0)	11.9	9.92	1.56	0.03	0.16
11	FFA(20:5)	4	0.36	0.59	0.4	0.32
12	FFA(28:0)	1.21	0.83	1.17	0.07	0.19
13	FFA(18:2)	31.39	5.89	1.78	0	0.04
14	FFA(20:4)	0.65	0.17	1.49	0.01	0.09
15	FFA(20:1)	7.43	3.27	0.62	0.82	0.47
16	FFA(22:0)	10.06	5.1	1.49	0.04	0.17
17	FFA(20:2)	0.29	0.12	0.05	0.24	0.26
18	FFA(26:0)	4.19	3.52	0.73	0.45	0.34
19	Total	4566.15	706.37			

high concentrations of FFA induced a diabetes-like environment (Wang et al., 2019). FFA is a cause of insulin resistance in obese people, insulin and free fatty acid (FFA) concentration in the rule of FFA metabolism (Capaldo et al., 1994; Gupta & Sharma, 2014). FFA 18:0 and FFA 16:0 were critical,as they are excipient-related degradation products in the liposomal formulation and may affect the safety and efficacy of the drug. FFA (18:1): identifies the specific FFAs that best predicts the occurrence of T2DM during obesity and assess their potential, identify the specific FFAs that best predicts the occurrence of T2DM during obesity and assess their potential application value (Ma et al., 2021).

Five DAG molecular species, namely, DAG (16:0/16:1) (0.39 µg/mL vs 0.35 µg/mL), DAG (16:1/16:1) (0.26 µg/mL vs 0.24 µg/mL) showed no significant difference between Canadian and Shangri-La icewine;DAG (16:0/16:0) (49.08 µg/mL vs 23.94 µg/mL), DAG (14:0/20:0) (0.24 µg/mL vs 0.14 µg/mL), DAG (16:0/18:0) (81.33 µg/mL vs 40.03 µg/mL), and Cer (18:1/24:1) (0.31 µg/mL vs 0.33 µg/mL) were significantly higher in Canadian icewine than in Shangri-La icewine;Total Canadian (131.24 µg/mL) icewine samples' DAG content was higher than Shangri-La icewine (64.67 µg/mL) (Table 5). Palmitate (C16:0) enhances proinflammatory IKK-NF kappa B signalling through a mechanism involving the MAP kinase (Raf-MEK-ERK) pathway, DAG-sensitive protein kinase C (PKC), RAF kinase inhibitory protein, and the structurally related monounsaturated fatty acid palmitoleate (C16:1) on pro-inflammatory signalling was investigated (Macrae et al., 2013). Palmitate DAG (14:0/20:0)—a versatile molecule that participates as a substrate in the synthesis of structural and energetic lipids and acts as a physiological signal that activates PKC-induced insulin resistance in human muscle related to alterations in DAG/PKC signalling—was investigated in normal volunteers

during euglycemic-hyperinsulinemic clamping in which there was an increase in obesity levels were increased by a lipid/heparin infusion (Itani et al., 2002; Macrae et al., 2013).

Only one N-palmitale-D-erythro-sphingosylphosphorylcholine molecular species was ascertained without significant differences between Shangri-La (8.15 µg/mL) and Canadian (0.31 µg/mL) icewine samples (Table 6). Sphingomyelin (SM) to ceramide (Cer) by the assembly of domains in giant unilamellar vesicles (Taniguchi et al., 2006). Six Cer molecular species, namely Cer (18:1/26:1) (0.39 µg/mL vs 0.35 µg/mL), Cer (18:1/26:0) (0.34 µg/mL vs 0.39 µg/mL), Cer (18:1/22:0) (0.14 µg/mL vs 0.13 µg/mL), Cer (18:1/24:0) (0.44 µg/mL vs 0.46 µg/mL), Cer (18:1/16:1) (0.25 µg/mL vs 0.18 µg/mL), and Cer (18:1/24:1) (0.31 µg/mL vs 0.33 µg/mL), were identified and quantified, and no significant difference was found between Shangri-la (0.39 µg/mL) and Canadian (0.35 µg/mL) icewine; Total Canadian icewine samples' Cer content was higher than that of Shangri-La icewine; however, no significant differences were found between Shangri-La and Canadian icewine (Table 6). Palmitoyl sphingomyelin (PSM) with phytosterol derivatives of β-sitosteryl glucoside palmitate (SGP), β-sitosteryl glucoside (SG) and β-sitosterol (SITO) (Sakamoto et al., 2013). Cer-C24:1 is related to stroke (Fiedorowicz et al., 2019). The overexpression of neutral ceramidase inhibited a tumour necrosis factor (TNF)-α-induced increased apoptosis in rat primary hepatocyte and C-ceramide (Strelow et al., 2000). Ceramide and sphingosine-1-phosphate/sphingosine act as Photodynamic and therapy-Elicited Damage-Associated Molecular Patterns (Korbelik et al., 2014; Nagayama & Katsuta, 2014). Ceramide is inhibited by reduced glutathione and ubiquinone (De Luca et al., 2005). Inhibitory effect of ceramide playing the roles in Ceramide-induced HCV entrance (Voisset et al., 2008).

Table 5. DAG lipids molecular species and content in icewine samples.

id	MS2 name	C-2016	Y-2016	VIP	P-VALUE	Q-VALUE
1	DAG(16:0/16:1)	0.32	0.32	0.17	0.99	0.51
2	DAG(16:0/16:0)	49.08	23.94	1.5	0.07	0.19
3	DAG(14:0/20:0)	0.24	0.14	1.26	0.03	0.15
4	DAG(16:0/18:0)	81.33	40.03	1.49	0.07	0.19
5	DAG(16:1/16:1)	0.26	0.24	0.63	0.84	0.47
6	Total	131.24	64.67			

Table 6. Cer and SM lipids molecular species and content in icewine samples.

id	MS2 name	C-2016	Y-2016	VIP	P-VALUE	Q-VALUE
1	Cer(18:1/26:1)	0.35	0.39	0.75	0.52	0.36
2	Cer(18:1/26:0)	0.34	0.39	0.72	0.51	0.35
3	Cer(18:1/22:0)	0.13	0.14	0.01	0.91	0.49
4	Cer(18:1/24:0)	0.46	0.44	0.54	0.89	0.49
5	Cer(18:1/16:1)	0.18	0.25	0.8	0.3	0.28
6	Cer(18:1/24:1)	0.33	0.31	0.64	0.79	0.46
7	SM(14:0)	8.15	0.31	0.45	0.5	0.35
8	Total	9.94	2.24			

4. Discussion

Lipid plays a crucial role in wine yeast fermentation. Non-Saccharomyces yeasts enhance contributions to wine traits, evolving lipid requirements and metabolism (Mbuyane et al., 2021). Lipids promoted acetic acid metabolism and thiol release (Deroite et al., 2018).Trans-Resveratrol demonstrated also a dose-dependent inhibition of PAF-induced platelet aggregation along with the already reported inhibitory activity against thrombin and adenosine-5'-diphosphate in red wine may (Fragopoulou et al., 2000). Results highlight that dietary lipids are crucial molecular agents impacting our sensory perception during wine consumption (Saad et al., 2021).

Lipids were an important constitution in food science, which plays multiple functions on food, nutrient, and human being health (Brahe et al., 2013). Lipid molecules imply massive biological matrices, lipids are an essential nutrient and flavour substances in icewine (Coelho et al., 2020). No qualitative and quantitative studies on lipids in icewine are available. Therefore, the current study aimed to comprehensively detecting the lipids in icewine from different regions using lipidomics technology to appricated the differences between the lipid composition of icewine from different areas and deepen the existing understanding of lipids icewine. In the present study, the identification, quantitative analysis, and comparison of lipid in icewine from different regions, such as Canada and Shangri-La, was performed. Lipids in the icewine indicates food are nutrients beneficial to human health.

Foodomics as a new and useful tool to study food chemistry and function, lipidomics as an effective method highlight the comprehensive analysis of molecules (Inoue & Toyo'oka, 2015). LC-QTOF-MS is an effective approach that detected lipid molecules in Icewine samples. In the current study, 142 lipids belonging to 5 classes, 102 TAG, 18 FFA, 5 DAG, 6 Cer, and 1 SM, were quantified. Shangri-la's total lipid molecular content (TAG and FFA)

was higher than Canada's. However, the DAG (16:0/16:1) content of total Canadian icewine samples (398.26 μg/mL) was higher than that of Shangri-La (522.43 μg/mL); the SM (14:0) content of Canada was higher than that of Shangri-La. Thus, Shangri-La icewine manifests more nutrients beneficial for human health than Canadian icewine. Human being were seeking more nutrient and health food. Icewine as a better choice, which specific nutrients and flavour food. In this study, thev landscape in Lipid molecules TAG, FFA, DAG, Cer, and SM, was quantified of Shangri-La and Canadian icewine samples.

Conflict of interest

No conflicts of interest were declared by all authors.

Acknowledgements

References

Boccard, J., & Rutledge, D. N. (2013). A consensus orthogonal partial least squares discriminant analysis (OPLS-DA) strategy for multiblock Omics data fusion. *Analytica Chimica Acta*, 769, 30-39. http://dx.doi.org/10.1016/j.aca.2013.01.022. PMid:23498118.

Brahe, L. K., Ängquist, L., Larsen, L. H., Vimaleswaran, K. S., Hager, J., Viguerie, N., Loos, R. J., Handjieva-Darlenska, T., Jebb, S. A., Hlavaty, P., Larsen, T. M., Martinez, J. A., Papadaki, A., Pfeiffer, A. F., van Baak, M. A., Sørensen, T. I., Holst, C., Langin, D., Astrup, A., & Saris, W. H. (2013). Influence of SNPs in nutrient-sensitive candidate genes and gene–diet interactions on blood lipids: the DiOGenes study. *British Journal of Nutrition*, 110(5), 790-796. http://dx.doi.org/10.1017/S0007114512006058. PMid:23360819.

Capaldo, B., Napoli, R., Di Marino, L., Guida, R., Pardo, F., & Saccá, L. (1994). Role of insulin and free fatty acid (FFA) availability on regional FFA kinetics in the human forearm. *The Journal of Clinical Endocrinology and Metabolism*, 79(3), 879-882. http://dx.doi.org/10.1210/jcem.79.3.8077375. PMid:8077375.

Chong, J., Soufan, O., Li, C., Caraus, I., Li, S., Bourque, G., Wishart, D. S., & Xia, J. (2018). MetaboAnalyst 4.0: towards more transparent and integrative metabolomics analysis. *Nucleic Acids Research*, 46(W1), W486-W494. http://dx.doi.org/10.1093/nar/gky310. PMid:29762782.

Coelho, A. L. S., Feuser, P. E., Carciofi, B. A. M., Oliveira, D., & Andrade, C. J. (2020). Biological activity of mannosylerythritol lipids on the mammalian cells. *Applied Microbiology and Biotechnology*, 104(20), 8595-8605. http://dx.doi.org/10.1007/s00253-020-10857-9. PMid:32875366.

Deroite, A., Legras, J. L., Rigou, P., Ortiz-Julien, A., & Dequin, S. (2018). Lipids modulate acetic acid and thiol final concentrations in wine during fermentation by Saccharomyces cerevisiae × Saccharomyces kudriavzevii hybrids. *AMB Express*, 8(1), 130. http://dx.doi.org/10.1186/s13568-018-0657-5. PMid:30097818.

Dunn, W., Broadhurst, D., Begley, P., Zelena, E., Francis-McIntyre, S., Anderson, N., Brown, M., Knowles, J. D., Halsall, A., Haselden, J. N., Nicholls, A. W., Wilson, I. D., Kell, D. B., & Goodacre, R. (2011). Procedures for large-scale metabolic profiling of serum and plasma using gas chromatography and liquid chromatography coupled to mass spectrometry. *Nature Protocols*, 6(7), 1060-1083. http://dx.doi.org/10.1038/nprot.2011.335. PMid:21720319.

Fiedorowicz, A., Kozak-Sykała, A., Bobak, Ł., Kałas, W., & Strządała, L. (2019). Ceramides and sphingosine-1-phosphate as potential markers in diagnosis of ischaemic stroke. *Neurologia i Neurochirurgia Polska*, 53(6), 484-491. http://dx.doi.org/10.5603/PJNNS.a2019.0063. PMid:31804702.

Fragopoulou, E., Nomikos, T., Antonopoulou, S., Mitsopoulou, C. A., & Demopoulos, C. A. (2000). Separation of Biologically Active Lipids from Red Wine. *Journal of Agricultural and Food Chemistry*, 48(4), 1234-1238. http://dx.doi.org/10.1021/jf990554p. PMid:10775377.

Ghareib, M., Youssef, K. A., & Khalil, A. A. (1988). Ethanol tolerance of Saccharomyces cerevisiae and its relationship to lipid content and composition. *Folia Microbiologica*, 33(6), 447-452. http://dx.doi.org/10.1007/BF02925769. PMid:3071514.

Gupta, M, & Sharma, N. (2014). Status of serum free fatty acid (FFA) level in obese person and its association with DM type-II. *International Journal of Research and Review*, 6(11), 245-248.

Inoue, K., & Toyoòka, T. (2015). Foodomics. In Y. Picó (Ed.), *Comprehensive Analytical Chemistry* (pp. 653-684). Amsterdam: Elsevier.

Itani, S. I., Ruderman, N. B., Schmieder, F., & Boden, G. (2002). Lipid-Induced Insulin Resistance in Human Muscle Is Associated With Changes in Diacylglycerol, Protein Kinase C, and IκB-α. *Diabetes*, 51(7), 2005-2011. http://dx.doi.org/10.2337/diabetes.51.7.2005. PMid:12086926.

Korbelik, M., Banáth, J., Zhang, W., Wong, F., Bielawski, J., & Separovic, D. (2014). Ceramide and sphingosine-1-phosphate/sphingosine act as photodynamic therapy-elicited damage-associated molecular patterns: release from cells and impact on tumor-associated macrophages. *Journal of Analytical & Bioanalytical Techniques*, (S1), 009. http://dx.doi.org/10.4172/2155-9872.S1-009.

Li, N., Wang, L., Yin, J., Ma, N., & Tao, Y. (2022). Adjustment of impact odorants in Hutai-8 rose wine by co-fermentation of Pichia fermentans and Saccharomyces cerevisiae. *Food Research International*, 153, 110959. http://dx.doi.org/10.1016/j.foodres.2022.110959. PMid:35227481.

Li, X., Wang, X., Li, H., Li, Y., & Guo, Y. (2021). Seminal plasma lipidomics profiling to identify signatures of Kallmann Syndrome.

Frontiers in Endocrinology, 12, 692690. http://dx.doi.org/10.3389/fendo.2021.692690. PMid:34393999.

De Luca, T., Morré, D. M., Zhao, H., & Morré, D. J. (2005). NAD+/NADH and/or CoQ/CoQH2 ratios from plasma membrane electron transport may determine ceramide and sphingosine-1-phosphate levels accompanying G1 arrest and apoptosis. *BioFactors*, 25(1-4), 43-60. http://dx.doi.org/10.1002/biof.5520250106. PMid:16873929.

Ma, Y., Xiong, J., Zhang, X., Qiu, T., Pang, H., Li, X., Zhu, J., Wang, J., Pan, C., Yang, X., Chu, X., Yang, B., Wang, C., & Zhang, J. (2021). Potential biomarker in serum for predicting susceptibility to type 2 diabetes mellitus: Free fatty acid 22:6. *Journal of Diabetes Investigation*, 12(6), 950-962. http://dx.doi.org/10.1111/jdi.13443. PMid:33068491.

Macrae, K., Stretton, C., Lipina, C., Blachnio-Zabielska, A., Baranowski, M., Gorski, J., Marley, A., & Hundal, H. S. (2013). Defining the role of DAG, mitochondrial function, and lipid deposition in palmitate-induced proinflammatory signaling and its counter-modulation by palmitoleate. *Journal of Lipid Research*, 54(9), 2366-2378. http://dx.doi.org/10.1194/jlr.M036996. PMid:23833248.

Mbuyane, L. L., Bauer, F. F., & Divol, B. (2021). The metabolism of lipids in yeasts and applications in oenology. *Food Research International*, 141, 110142. http://dx.doi.org/10.1016/j.foodres.2021.110142. PMid:33642009.

Olsvik, P. A., & Søfteland, L. (2020). Mixture toxicity of chlorpyrifos-methyl, pirimiphos-methyl, and nonylphenol in Atlantic salmon (Salmo salar) hepatocytes. *Toxicology Reports*, 7, 547-558. http://dx.doi.org/10.1016/j.toxrep.2020.03.008. PMid:32373476.

Phan, Q., & Tomasino, E. (2021). Untargeted lipidomic approach in studying pinot noir wine lipids and predicting wine origin. *Food Chemistry*, 355, 129409. http://dx.doi.org/10.1016/j.foodchem.2021.129409. PMid:33799257.

Saad, A., Bousquet, J., Fernandez-Castro, N., Loquet, A., & Géan, J. (2021). New insights into wine taste: impact of dietary lipids on sensory perceptions of grape tannins. *Journal of Agricultural and Food Chemistry*, 69(10), 3165-3174. http://dx.doi.org/10.1021/acs.jafc.0c06589. PMid:33655748.

Sakamoto, S., Nakahara, H., & Shibata, O. (2013). Miscibility behavior of sphingomyelin with phytosterol derivatives by a Langmuir Monolayer approach. *Journal of Oleo Science*, 62(10), 809-824. http://dx.doi.org/10.5650/jos.62.809. PMid:24088519.

Siriwardane, D. A., Wang, C., Jiang, W., & Mudalige, T. (2020). Quantification of phospholipid degradation products in liposomal pharmaceutical formulations by ultra performance liquid chromatography-mass spectrometry (UPLC-MS). *International Journal of Pharmaceutics*, 578, 119077. http://dx.doi.org/10.1016/j.ijpharm.2020.119077. PMid:31988036.

Srisamatthakarn, P. (2011). *Improvement of varietal aroma in grape and tropical fruit wines by optimal choice of yeasts and nutrient supplements*. Giessen: Justus-Liebig-Universität Gießen.

Strelow, A., Bernardo, K., Adam-Klages, S., Linke, T., Sandhoff, K., Krönke, M., & Adam, D. (2000). Overexpression of acid ceramidase protects from tumor necrosis factor–induced cell death. *The Journal of Experimental Medicine*, 192(5), 601-612. http://dx.doi.org/10.1084/jem.192.5.601. PMid:10974027.

Taniguchi, Y., Ohba, T., Miyata, H., & Ohki, K. (2006). Rapid phase change of lipid microdomains in giant vesicles induced by conversion of sphingomyelin to ceramide. *Biochimica et Biophysica Acta*, 1758(2), 145-153. http://dx.doi.org/10.1016/j.bbamem.2006.02.026. PMid:16580624.

Tu, J., Yin, Y., Xu, M., Wang, R., & Zhu, Z. J. (2017). Absolute quantitative lipidomics reveals lipidome-wide alterations in aging brain. *Metabolomics*, 14(1), 5. http://dx.doi.org/10.1007/s11306-017-1304-x. PMid:30830317.

Voisset, C., Lavie, M., Helle, F., Op De Beeck, A., Bilheu, A., Bertrand-Michel, J., Tercé, F., Cocquerel, L., Wychowski, C., Vu-Dac, N., & Dubuisson, J. (2008). Ceramide enrichment of the plasma membrane induces CD81 internalization and inhibits hepatitis C virus entry. *Cellular Microbiology*, 10(3), 606-617. http://dx.doi.org/10.1111/j.1462-5822.2007.01070.x. PMid:17979982.

Wang, X., Huang, H., Su, C., Zhong, Q., & Wu, G. (2019). Cilostazol ameliorates high free fatty acid (FFA)-induced activation of NLRP3 inflammasome in human vascular endothelial cells. *Artificial Cells, Nanomedicine, and Biotechnology*, 47(1), 3704-3710. http://dx.doi.org/10.1080/21691401.2019.1665058. PMid:31514535.

Want, E. J., Wilson, I. D., Gika, H., Theodoridis, G., Plumb, R. S., Shockcor, J., Holmes, E., & Nicholson, J. K. (2010). Global metabolic profiling procedures for urine using UPLC–MS. *Nature Protocols*, 5(6), 1005-1018. http://dx.doi.org/10.1038/nprot.2010.50. PMid:20448546.

Wu, B., Wei, F., Xu, S., Xie, Y., Lv, X., Chen, H., & Huang, F. (2021). Mass spectrometry-based lipidomics as a powerful platform in foodomics research. *Trends in Food Science & Technology*, 107, 358-376. http://dx.doi.org/10.1016/j.tifs.2020.10.045.

Youngtaek, O. H., Kisook, O. H., & Kang, I. (1986). 24-h continuous nicotinic acid infusion causes FFA rebound and insulin resistance in rats. *SEG Technical Program Expanded Abstracts*, 12, 715.

Highlights

- First to use lipidomics approach to study icewine lipids.
- First to quantitatively analyse lipid content in icewine from Canada and China.
- Advances in analytical techniques and bioinformatics strategie stactic will expand the applications of lipidomics in food science.

Abbreviations

UPLC-QTOF-MS: Ultra High Performance Liquid TandemChromatography Quadrupole Time-of-Flight Mass Spectrometry

TAG: Triacylglycerol

DAG: Diacylglycerol

FFA: Free fatty acid

CER: Ceramides and sphingosine-1-phosphate

SM (14:0): N-palmitoyl-D-erythro-sphingosylphosphorylcholine

Supplementary material

Table S1 - Icewine samples come from Canadian and Shangri-La of Yunnan.

Table S2 - Icewine lipids sample composition difference for Canadian and Shangri-La of Yunnan.

Table S3 - Relationships between icewine lipids composition.

Table S4 - Icewine lipids composition and contents for Canadian and Shangri-La of Yunnan.

Table S5 - Matrix of Radarplot Analysis

Table S6 - Icewine lipids composition and contents Ori database for Canadian and Shangri-La of Yunnan.

Table S7 - Icewine lipids composition and contents Ori datas analysts for Canadian and Shangri-La of Yunnan.

Table S8 - Calcification of icewine lipids and annotation.

Table S9 - Relationships between icewine lipids composition.

Table S10 - OPLS-DA Model explantation and annotation.

This material is available as part of the online article from https://doi.org/10.5327/fst.94822